ISPRS Journal of Photogrammetry and Remote Sensing 130 (2017) 370–384

Contents lists available at ScienceDirect

ISPRS Journal of Photogrammetry and Remote Sensing

journal homepage: www.elsevier.com/locate/isprsjprs

Change detection using landsat time series: A review of frequencies, preprocessing, algorithms, and applications

Zhe Zhu *

Department of Geosciences, Texas Tech University, Lubbock, TX 79409, United States
Center for Geospatial Technology, Texas Tech University, Lubbock, TX 79409, United States
Climate Science Center, Texas Tech University, Lubbock, TX 79409, United States

ARTICLE INFO

Article history:
Received 8 February 2017
Received in revised form 30 June 2017
Accepted 30 June 2017
Available online 11 July 2017

Keywords:
Review
Landsat
Change detection
Time series

ABSTRACT

The free and open access to all archived Landsat images in 2008 has completely changed the way of using Landsat data. Many novel change detection algorithms based on Landsat time series have been developed We present a comprehensive review of four important aspects of change detection studies based on Landsat time series, including frequencies, preprocessing, algorithms, and applications. We observed the trend that the more recent the study, the higher the frequency of Landsat time series used. We reviewed a series of image preprocessing steps, including atmospheric correction, cloud and cloud shadow detection, and composite/fusion/metrics techniques. We divided all change detection algorithms into six categories, including thresholding, differencing, segmentation, trajectory classification, statistical boundary, and regression. Within each category, six major characteristics of different algorithms, such as frequency, change index, univariate/multivariate, online/offline, abrupt/gradual change, and sub-pixel/pixel/spatial were analyzed. Moreover, some of the widely-used change detection algorithms were also discussed. Finally, we reviewed different change detection applications by dividing these applications into two categories, change target and change agent detection.

Contents

1. Introduction . . . 371
2. Frequencies . . . 372
3. Preprocessing . . . 373
   3.1. Atmospheric correction . . . 373
   3.2. Cloud and cloud shadow detection . . . 373
   3.3. Composite, fusion, and metrics . . . 374
4. Algorithms . . . 375
   4.1. Thresholding . . . 377
   4.2. Differencing . . . 377
   4.3. Segmentation . . . 378
   4.4. Trajectory classification . . . 378
   4.5. Statistical boundary . . . 378
   4.6. Regression . . . 378
   4.7. Some of the widely-used algorithms . . . 379
5. Applications . . . 380
   5.1. Change target . . . 380
   5.2. Change agent . . . 380

* Address: Department of Geosciences, Texas Tech University, Lubbock, TX 79409, United States.
E-mail address: zhe.zhu@ttu.edu

http://dx.doi.org/10.1016/j.isprsjprs.2017.06.013

6. Conclusions . . . 380
Acknowledgements . . . 381
References . . . 381

1. Introduction

Landsat data have been used to study how the Earth's surface has been changing for decades due to its long history and relatively high spatial resolution (Kennedy et al., 2014). However, for a long time, Landsat data have rarely been used for time series analysis, due to the high cost (Loveland and Dwyer, 2012) and the need for large storage and high-performance computing capabilities (Hansen and Loveland, 2012). Historically, change detection using Landsat data was mainly based on comparing images at two different times – the bitemporal approach (Singh, 1989). Although the bitemporal approach is mathematically simple and does not need to store large amount of data, it is less useful compared to the time series approach that is able to provide more comprehensive understanding of the complexity of the Earth's surface dynamics (Coppin et al., 2004). In recent decades, the cost of data storage has decreased dramatically, and we have witnessed an overwhelming increase in computing power, which provide the foundation for time series analysis suing Landsat data. In 2008, the free and open access to the whole Landsat archive has further revolutionized the way of using Landsat data (Woodcock, 2008; Wulder et al., 2012). Many studies used Landsat time series, and a majority of them were focused on change detection (Banskota et al., 2014).

Recently, with the Landsat Global Archive Consolidation (LGAC) initiative, more than 3.2 million Landsat images have been added to the archive located at the U.S. Geological Survey (USGS) Earth Resources Observation and Science (EROS) Center (Wulder et al., 2016). This has made time series analysis with Landsat data possible for places previously characterized by an insufficient density of Landsat time series. Though the Scan Line Corrector (SLC)-off on Landsat 7 has greatly impacted the use of Landsat data, it has limited influence on time series analysis. Basically, we can treat those SLC-off areas the same as clouds or cloud shadows and use what is left for time series analysis for each individual pixel (Zhu and Woodcock, 2014a, 2014b). The launch of Landsat 8 in 2013 has filled the role of the long-lasting Landsat 5 and compared to the previous Landsat satellites Landsat 8 is collecting way more images (Roy et al., 2014), at a substantially higher signal to noise ratio (Schott et al., 2016). All of these factors have made time series analysis with Landsat data one of the top research topics in the remote sensing community.

Remote sensing change detection is the process of identifying differences between images at different times (Singh, 1989). In this process, seasonal differences caused by solar angle differences and vegetation phenological changes are usually seen as the major sources of noise in change detection and need to be avoided by selecting images from the same season or corrected based on some de-seasoning methods. In this review, we will only focus on studies that detect changes that are non-seasonal. Though plenty of literature reviews already exist on change detection using remote sensing data, most of them only reviewed methods that use two dates of images (Singh, 1989; Coppin et al., 2004; Lu et al., 2004). Recently, some reviews discussed change detection algorithms based on time series of satellite data, but they were either only concentrated on detecting forest change (Banskota et al., 2014; Thonfeld et al., 2015) or were not Landsat data specific (Boriah, 2010; Thonfeld et al., 2015).

Based on a literature search within Scopus, the largest abstract and citation database of peer-reviewed literature, the number of publications on "change detection", "Landsat", and "time series" has increased dramatically after the opening of Landsat archive for free access in 2008, and the increase is particularly noticeable in that year (Fig. 1). This suggests that change detection using Landsat time series has become a more important field in remote sensing. Table 1 lists top 15 most relevant journals, most prolific authors, and major research institutions within this field. Note that the search within Scopus provided a total of 254 articles, but some of them are not change detections based on Landsat time series or are published later than the submission date of this review (we excluded them in this review). Moreover, we also found some articles that are actually detecting change with Landsat time series but are not included in Scopus (we added them in this review). In this paper, we provided a comprehensive review of four important aspects, including frequencies, preprocessing, algorithms, and

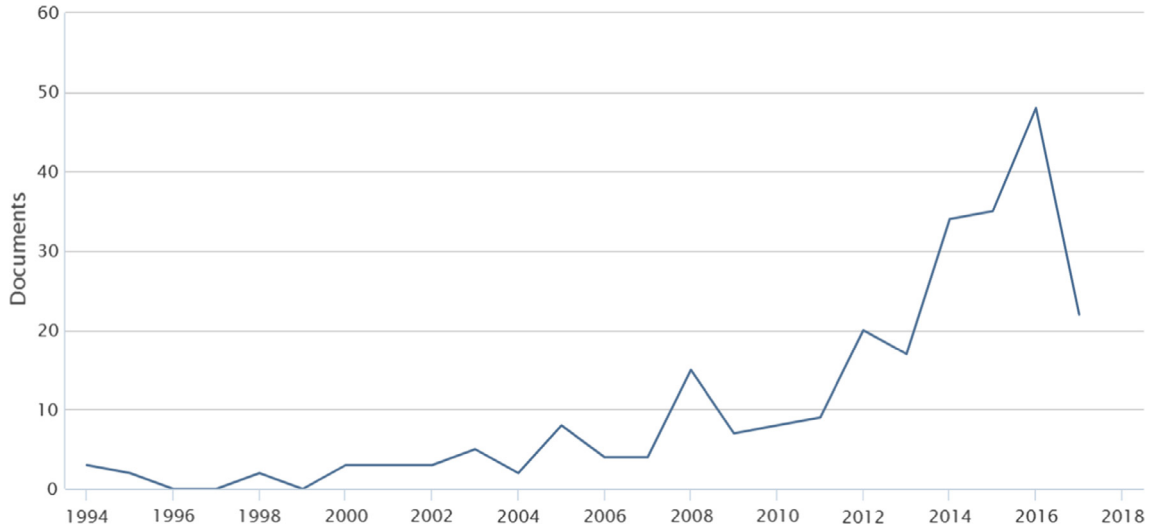

Fig. 1. Yearly publications from 1994 to 2017 indexed by Scopus. The Search was conduction on June 27, 2017 by search "change detection", "Landsat", and "time series" in article tile, abstract, and keywords. A total of 254 articles were found (document type only included research article).

Table 1
Top 15 most relevant journals, most prolific authors, and major research institutions from 1994 to 2017 indexed by Scopus. The numbers in the parentheses represent the total number of publications found in each category. The Search was conduction on June 27, 2017 by searching "change detection", "Landsat", and "time series" in article tile, abstract, and keywords. A total of 254 articles were found (document type only included research article).

Most Relevant Journals	Most Prolific Authors	Major Research Institutions
Remote Sensing of Environment (79)	Wulder, M.A. (15)	USDA Forest Service (19)
Remote Sensing (17)	Coops, N.C. (14)	Oregon State University (19)
International Journal of Remote Sensing (17)	Cohen, W.B. (13)	University of Maryland (16)
IEEE Transactions on Geoscience and Remote Sensing (9)	Yang, Z. (12)	Canadian Forest Service (15)
ISPRS Journal of Photogrammetry and Remote Sensing (7)	Kennedy, R.E. (12)	The University of British Columbia (15)
IEEE Journal of Selected Topics in Applied Earth Observations and Remote Sensing (6)	White, J.C. (9)	Chinese Academy of Sciences (12)
Forests (5)	Hermosilla, T. (7)	Boston University (12)
Forrest Ecology and Management (5)	Herold, M. (7)	NASA Goddard Space Flight Center (11)
Photogrammetric Engineering and Remote Sensing (4)	Huang, C. (7)	USDA ARS Corvallis Forestry Sciences Laboratory (11)
Journal of Applied Remote Sensing (4)	Sader, S.A. (7)	United States Geological Survey (9)
International Journal of Applied Earth Observation and Geoinformation (4)	Verbesselt, J. (7)	University of Maine (8)
Environmental Monitoring and Assessment (4)	Zhu, Z. (7)	Humboldt-University zu Berlin (7)
Canadian Journal of Remote Sensing (4)	Kuemmerle, T. (6)	Ministry of Education China (7)
Applied Geography (4)	Hostert, P. (5)	Wageningen University and Research Centre (7)
Sustainability Switzerland (3)	Radeloff, V.C. (5)	South Dakota State University (7)

applications for a total of 102 articles that used Landsat time series for change detection published between 2000 and 2016.

2. Frequencies

The Frequencies of Landsat time series used for change detection have increased substantially in the recent years. A single Landsat satellite visits the same location in every 16 days, which means it can collect 22–23 images per year for a given location (without considering overlap areas). Two Landsat satellites can provide a maximum of 45–46 images per year for the same location. Among the 102 articles that use Landsat time series for change detection, 89 of them contain the information to calculate the number of images used per year (Fig. 2). For those studies with multiple frequencies of Landsat time series, we used the highest frequency to represent the studies. If the study only provided a total number of Landsat images for several path/rows, we used the average frequency (across several path/rows) to represent the frequency of the study. Based on the statistics in Fig. 2, it is rare to see articles that used more than one Landsat image per year before 2008; in fact, many of them were using one Landsat images every two (0.5 images per year) or four years (0.25 images per year). After 2008, the story changed completely. We not only observed more articles (Fig. 1), but also observed a substantial increase in the number of Landsat images used per year in each article (Fig. 2). Studies that used one Landsat image per year or even 20–30 images per year appeared (Fig. 2A). As most of the time series studies were only interested in producing annual or biannual change maps, they tended to select multiple images (partly cloudy images)

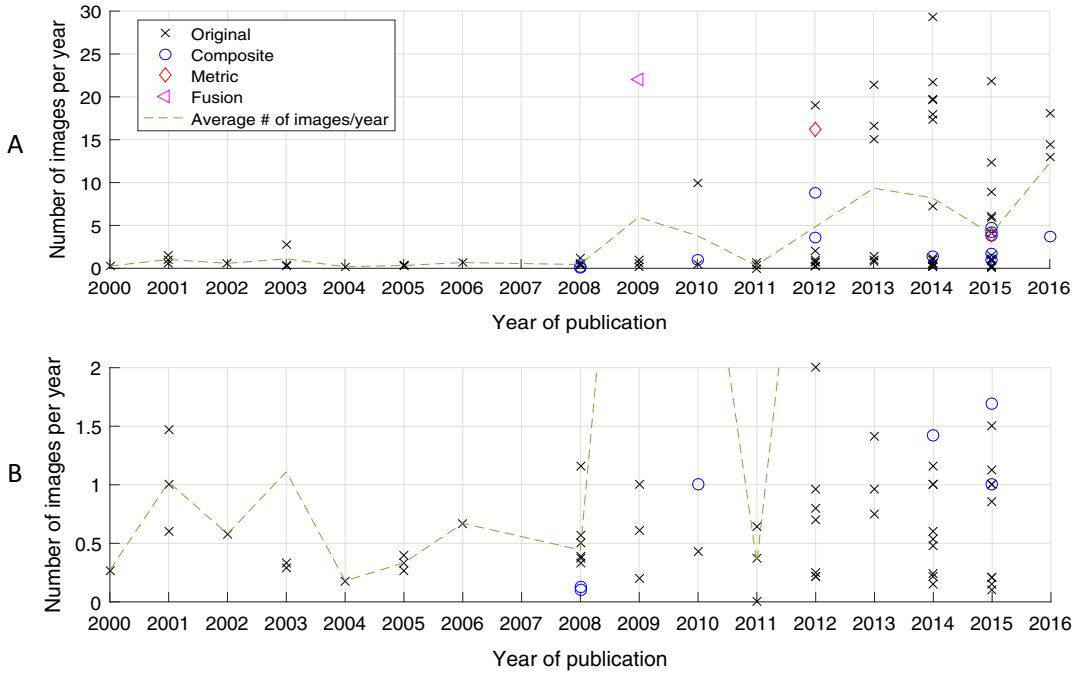

Fig. 2. Frequencies of Landsat time series used for change detection. The upper image (Figure A) shows the number of Landsat images used per year for all 89 articles. The lower image (Figure B) shows the number of Landsat images used per year for all 89 articles with the number of Landsat images used per year less or equal to 2. The "crosses" are the articles that used the original Landsat images as their inputs. The "circles" are the articles that used composite Landsat images as their inputs. The "diamonds" are the articles that used statistical metrics as their inputs. The "triangles" are the articles that used image fusion of Landsat and MODIS images as their inputs. The "dashed line" is the average values of number of Landsat images used per year from all the articles published in the same year.

acquired in the same season and the same year to produce cloud-free composite images as their inputs ("circles" in Fig. 2). In this way, seasonal differences caused by solar angle differences and vegetation phenological changes were minimized, and the data volume was reduced substantially. There are also studies that fused Landsat data with MODIS data and were capable of predicting Landsat image in every 16 days (22 images per year) for detecting forest change (Hilker et al., 2009) ("triangles" in Fig. 2A). After 2012, the average number of Landsat images used per year is approximately 10 ("dashed line" in Fig. 2) – another big increase compared to 2008. In 2012, new approaches that used all available Landsat images appeared in the literature ("crosses" in Fig. 2). These approaches can model the intra-annual seasonal changes in the time series and detect change as quick as every 8 days (Zhu et al., 2012). Note that there are also approaches that used statistical metrics, such as percentiles and slopes, as inputs for change detection ("diamonds" in Fig. 2). It is obvious that the more the recent the study, the more frequent the Landsat time series used. The use of more frequent Landsat time series provides the possibility of detecting change at a much faster pace. The dense Landsat time series also provides the possibility of capturing the intra-annual seasonal changes, and this information can be very helpful for improving change detection accuracy.

3. Preprocessing

Before applying different change detection algorithms for Landsat time series, we need to perform a series of image preprocessing steps, including atmospheric correction, cloud and cloud shadow detection, and composite/fusion/metrics. To make sure the time series are well aligned, most of the change detection algorithms only select Level 1 terrain-corrected (L1T) Landsat images as their inputs. The L1T Landsat images are reported to have high geometric accuracies (RMSE less than 30 meters in more than 99 percent of the data; http://landsat.usgs.gov/geometry.php), and geometric correction is generally considered unnecessary if only L1T Landsat images are included in change detection (Zhu and Woodcock, 2014a). Moreover, in 2016, the USGS EROS Center started reorganizing the Landsat archive into a formal tiered data Collection structure, which ensures that Landsat Level-1 products provides a consistent archive of known data quality (Tier 1, Tier 2, and Real-Time) to support time series analyses and data "stacking". Highest available data quality Landsat images (image-to-image tolerances of <12 m RMSE; https://landsat.usgs.gov/landsat-collections) are placed into Tier 1 and are considered most suitable for time series analysis.

3.1. Atmospheric correction

To reduce influences from atmosphere, atmospheric correction is a common preprocessing step before detecting change. Generally, there are two categories of atmospheric correction approaches: (1) relative normalization (Schroeder et al., 2006) and absolute correction (Chávez, 1996; Song and Woodcock, 2003). Relative normalization involves adjusting the radiometric of Landsat time series to a reference image based on the relationship between pseudo-invariant features from multi-date images (Song et al., 2001). Absolute correction can be further divided into two categories: empirical and physical-based approaches. The Dark-Object Subtraction (DOS) method is a widely used empirical method for estimating the path radiance based on the darkest value in the image (Song and Woodcock, 2003). DOS is relatively simple, but it does not consider the pixel-to-pixel variation in atmospheric effects. The physical-based approaches, such as Atmospheric/Topographic CORrection (ATCOR; Richter, 1997), MODerate resolution atmospheric TRANsmission (MODTRAN; Berk et al., 1998), and the Satellite Signal in the Solar Spectrum (6S) code (Vermote et al., 1997), are able to consider the heterogeneity of the atmosphere, but need many complicated steps and manual operations, which make them difficult to process large amount of Landsat time series. However, the Landsat Ecosystem Disturbance Adaptive Processing System (LEDAPS) software (Masek et al., 2006), which has adopted the 6S code, has made atmospheric correction for Landsats 4–7 fully automated. Recently, Vermote et al. (2016) developed an improved atmospheric correction algorithm for Landsat 8 (L8SR), which has shown an improvement over the ad-hoc Landsats 5–7 LEDAPS product. In 2012, Landsats 4–7 surface reflectance product generated from LEDAPS were provided by the USGS EROS Center. Later in 2014, provisional Landsat 8 surface reflectance products generated from L8SR were also provided by the USGS EROS Center. The free distribution of Landsat surface reflectance has greatly increased the use of LEDAPS- and L8SR-based surface reflectance products in change detection with Landsat time series ("dashed line" in Fig. 3).

3.2. Cloud and cloud shadow detection

The presence of clouds and their shadows complicate the use of Landsat data, making the detection of both items an evitable step prior to change detection. For a long time, cloud and cloud shadow detection at pixel level only existed for coarse spatial resolution sensors, such as Advanced Very High Resolution Radiometer (AVHRR) and Moderate Resolution Imaging Spectroradiometer

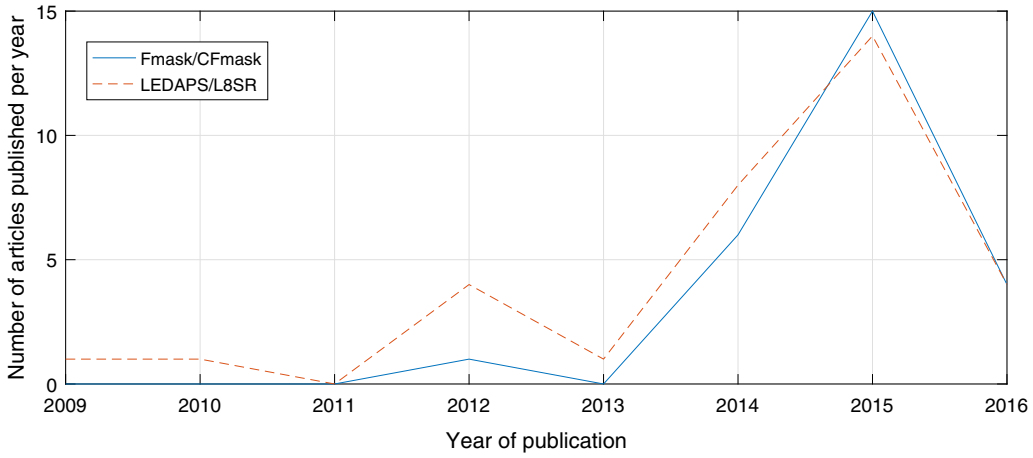

Fig. 3. Number of articles that used Fmask/CFmask ("dashed line") or LEDAPS/L8SR ("solid line") per year between 2009 and 2016. The statistics is derived from the 102 articles that used Landsat time series to detect change.

(MODIS) (Ackerman et al., 1998; Derrien et al., 1993; Saunders and Kriebel, 1988). Though Landsat has been collecting data for decades, there is hardly any operational algorithm that is capable of providing cloud and cloud shadow masks at pixel level. The Automated Cloud Cover Assessment (ACCA) system (Irish, 2000; Irish et al., 2006) works well for estimating the percentage of cloud cover for each individual Landsat image, but it does not provide clouds and cloud shadows masks for every Landsat pixel.

Since the free access to the entire Landsat archive in 2008, many cloud and cloud shadow detection algorithms have been developed based on a single-date Landsat image (Braaten et al., 2015; Huang et al., 2010b; Oreopoulos et al., 2011; Potapov et al., 2011; Roy et al., 2010; Scaramuzza et al., 2012; Qiu et al., 2017; Vermote et al., 2016; Vermote and Saleous, 2007; Zhu and Woodcock, 2014b, 2012). Most of the algorithms are designed for Thematic Mapper (TM) and Enhanced Thematic Mapper Plus (ETM+), and only a few algorithms are designed for Operational Land Imager (OLI)/Thermal Infrared Sensor (TIRS) (Scaramuzza et al., 2012; Vermote et al., 2016; Zhu et al., 2015a), and Multispectral Scanner (MSS) (Braaten et al., 2015). Though all the algorithms are developed for the same purpose, the mechanism for identifying clouds and their shadows are quite different. Generally, we can divide the algorithms into two categories: physical rules based and machine learning based algorithms.

The physical rule based algorithms detect clouds and their shadows based on their physical characteristics (Braaten et al., 2015; Huang et al., 2010b; Oreopoulos et al., 2011; Qiu et al., 2017; Vermote et al., 2016; Vermote and Saleous, 2007; Zhu and Woodcock, 2014b, 2012). Vermote and Saleous (2007) proposed a cloud and cloud shadow detection algorithm for Landsat data as one of the internal products in the LEDAPS software. This algorithm needs other auxiliary data like surface temperature from the National Centers for Environmental Prediction (NCEP) to generate a surface temperature reference layer for detecting clouds. Later, Vermote et al. (2016) proposed a cloud and cloud shadow detection algorithm for Landsat 8 data within the L8SR framework, which takes the advantages of some of the new spectral bands (e.g., the cirrus band and the new blue band). Huang et al. (2010b) proposed an algorithm that detects clouds based on temperature that are normalized by DEM and pre-classified confident forest pixels, and the cloud shadows are detected based on the solar-sensor geometry. Oreopoulos et al. (2011) modified a cloud detection algorithm that was originally developed for MODIS (Luo et al., 2008), and applied the algorithm to Landsat data. This algorithm performs on par with the ACCA algorithm, without using the thermal band. Zhu and Woodcock (2012) and Zhu et al. (2015b) proposed a method called Fmask (Function of mask) to detect cloud, cloud shadow, and snow in Landsats 4–8 images based on the spectral and spatial information in the Landsat data. Clouds are identified based on a cloud probability layer and a scene-based dynamic threshold, and cloud shadows are matched with clouds based on similarity and the corresponding solar-sensor geometry. Recently, Qiu et al. (2017) integrated DEM with the Fmask algorithm and developed a MFmask (Mountainous Fmask) algorithm that showed better cloud and cloud shadow detection results in mountainous regions. In 2013, the Fmask algorithm has been reprogramed in C (CFMask) by the USGS EROS Center, and the CFMask results are distributed by the USGS EROS Center along with the surface reflectance product. This free distribution of CFMask results has greatly increased the use of the Fmask algorithm, and we can see a dramatic increase in using Fmask/CFMask in change detection using Landsat time series since 2013 ("solid line" in Fig. 3). Moreover, within the formal tiered data Collection structure provided by USGS in 2016, the CFmask algorithm is used to provide the Quality Assessment (QA) band for all Collection 1 products. Cloud and cloud shadow detection in Landsat MSS images is quite challenging, as MSS does not have thermal and SWIR bands, both of which are critical in cloud detection. However, Braaten et al. (2015) used a rule-based approach to detect both clouds and cloud shadows in Landsat MSS images, and achieved comparable accuracies to the Fmask algorithm.

The machine learning based algorithms identify cloud and cloud shadow using a supervised classifier trained by previously collected training data (Hughes and Hayes, 2014; Potapov et al., 2011; Roy et al., 2010; Scaramuzza et al., 2012). Roy et al. (2010) and Potapov et al. (2011) used decision tree classifier to classify clouds and the classifiers were trained based on many manually interpreted cloud masks. Scaramuzza et al. (2012) developed two algorithms for detecting clouds based on Landsat 8 OLI (without using TIRS bands), with one from an off-the-shelf machine learning package (See5) and the other based on ACCA but enhanced by a neural network (AT-ACCA). Both algorithms have shown good accuracies and neither of them needs the thermal band as input. Hughes and Hayes (2014) also explored the use of a neural network classifier and spatial post-processing to identify clouds and cloud shadows in Landsat images. Compared to the Fmask algorithm, this approach achieved lower omission errors in cloud shadow detection and slightly higher omission errors in cloud detection. Though all these studies pointed out the usefulness of machine learning based algorithms for cloud and cloud shadow detection, these algorithms require a certain level of knowledge of clouds, cloud shadows, and land surface condition within the image (as the training data) and these algorithms can easily fail to detect cloud and cloud shadow for certain unique conditions (Huang et al., 2010b).

The recent progress of the fully automated cloud and cloud shadow detection algorithms based on a single-date Landsat image has facilitated many remote sensing applications that need to process large number of Landsat images. However, for change detection using Landsat time series, the accuracy of single-date algorithms remains insufficient. To further improve cloud and cloud shadow detection accuracies, algorithms based on multitemporal Landsat images have been developed. Jin et al. (2013) and Wang et al. (1999) proposed to detect clouds and their shadows by comparing a cloud-free reference image to the observed images. This approach is relatively simple and can provide accurate results, but it is highly dependent on the availability and quality of the reference image, which makes it difficult to work operationally. Recently, cloud and cloud shadow detection algorithms based on Landsat time series have been developed, which are able to provide accurate detection results, and at the same time fully automated (Goodwin and Collett, 2014; Hagolle et al., 2010; Zhu and Woodcock, 2014b). One disadvantage of these time series algorithms is that they may also identify some ephemeral changes (e.g., soil wetness change) as clouds or cloud shadows (Zhu and Woodcock, 2014b). Considering the importance of accurate cloud and cloud shadow detection in analyzing Landsat time series, more time series based cloud and cloud shadow detection algorithms are anticipated in the near future.

3.3. Composite, fusion, and metrics

Before detecting change, some algorithms need to create cloud-free composite Landsat images, fuse Landsat images with other low spatial resolution images, or calculate statistical metrics from the Landsat time series.

Image compositing is a good tool for reducing data volume and minimizing atmosphere influences, but most of the image compositing algorithms are only designed for coarse spatial resolution images, such as AVHRR (Holben, 1986) and MODIS (Luo et al., 2008), with only a few studies that are designed for Landsat (Griffiths et al., 2013; Potapov et al., 2011; Roy et al., 2010;

White et al., 2014; Zhu et al., 2015b). Roy et al. (2010) first proposed an image composite method for Landsat ETM+ images mainly based on a combination of maximum Normalized Difference Vegetation Index (NDVI) and highest brightness temperature criteria. This method has been applied to the entire conterminous U.S. and the final composites are provided for free download. Potapov et al. (2011) used the median values of the Near Infrared (NIR) band as the criteria for selecting the "best" observations and this approach performed better than the conventional maximum NDVI compositing method. Griffiths et al. (2013) developed a method that calculates scores for every Landsat observation, with image compositing rules determined by the weighted scores that are calculated based on acquisition year, acquisition day of year, distance of a given pixel to cloud (from Fmask). Similarly, White et al. (2014) proposed a pixel-based image compositing method that calculates pixel scores based on sensor type, day of year, distance to cloud or cloud shadow (from Fmask), and opacity (from LEDAPS). Zhu et al. (2015b) proposed to use all available clear Landsat data to estimate time series models for each pixel and each spectral band, and used the estimated time series models to predict daily clear-sky synthetic Landsat data. Among all these methods, it is hard to quantify which method works the best, as there is not a standard set of reference images to compare with. Most of the evaluations are made by visual check of the results based on natural color composite.

As the frequency of Landsat time series is relatively low, it may take a few weeks or months to generate cloud-free composite Landsat images, and the "best" observations selected from image compositing may show large seasonal differences. To overcome this limitation, fusing Landsat data with coarse resolution images, such as MODIS data provides a solution (Gao et al., 2006; Hilker et al., 2009; Roy et al., 2008; Zhu et al., 2010). Gao et al. (2006) proposed the Spatial and Temporal Adaptive Reflectance model (STARFM), which is capable of predicting Landsat-scale observations on MODIS observation dates. STARFM has been later modified to form the Spatial Temporal Adaptive Algorithm for mapping Reflectance Change (STAARCH) for detecting forest disturbance (Hilker et al., 2009), and the Enhanced STARFM (ESTARFM) for better handling of heterogeneous areas (Zhu et al., 2010). Gao et al. (2015) reviewed STARFM, STAARCH, and ESTARFM, and suggested that though these approaches can produce images with high spatial temporal resolution, they are still dependent on the availability of actual satellite images and the quality of the remote sensing products, therefore, cannot replace the actual satellite missions. Roy et al. (2008) proposed a semi-physical fusion approach that uses MODIS Bidirectional Reflectance Distribution Function (BRDF)/Albedo land surface characterization products to predict Landsat images, and achieved good results. The synthetic Landsat images generated by fusing Landsat and MODIS can substantially densify the Landsat time series, which can be critical for time series analysis in places that are frequently covered by clouds.

Metrics from Landsat time series can provide extra generic feature space, which is particularly useful for the multi-date classification change detection method (Hansen et al., 2014, 2013; Potapov et al., 2011, 2015, 2012). There are many kinds of metrics that can be derived from Landsat time series, such as individual ranks, means, and regression slopes of spectral bands and vegetation indices, and they are generally calculated either based on time-sequential reflectance or reflectance ranking. One advantage of this method is that the statistics derived from Landsat time series are relatively robust to noise and contains temporal information that are important inputs for multi-date classification change detection method.

4. Algorithms

Based on the mathematical approach used for detecting change, the Landsat time series change detection algorithms can be divided into six major categories, including thresholding, differencing, segmentation, trajectory classification, statistical boundary, and regression (Fig. 4 and Table 2). Within each category, six characteristics, including frequency, change index, univariate/multivariate, online/offline, abrupt/gradual change, and sub-pixel/pixel/spatial were discussed. The detailed definitions of these characteristics are as follows.

Frequency: Number of Landsat images used for the same location. We used three levels to indicate the frequency of Landsat data used: low (a few years per image), medium (approximately 1 images per year), and high (more than 1 images per year). Algorithms that use multiple cloudy Landsat images per year to derive annual cloud-free composite images are categorized into medium frequency.

Change index: The index used for detecting change, such as spectral bands, vegetation indices, tasseled cap transformations, land cover class, or land cover fractions.

Univariate/multivariate: Most of the change detection algorithms use a single variable at each time point (univariate), but there are some algorithms use multivariate vector at each time point (multivariate).

Online/offline: Online change detection assumes the time series data are coming in at a certain rate, and the main goal is to detect changes in near real-time (or continuously), with minimum delay. Offline change detection assumes the time series data already exist and the main goal is to detect when the characteristics of the time series changed.

Abrupt/gradual change: Abrupt change refers to large magnitude changes which are usually occurred in a short time. Abrupt change can be caused by disturbances such as deforestation, floods, fires, or urbanization. Gradual change refers to small magnitude changes which are usually occurred in a long time. Gradual change can be triggered by factors, such as interannual climate variability or gradual change in land management or land degradation.

Subpixel/pixel/spatial: Most of algorithms use pixel as their smallest unit (pixel), but there are some algorithms use sub-pixel information to detect change (subpixel). Most of the algorithms

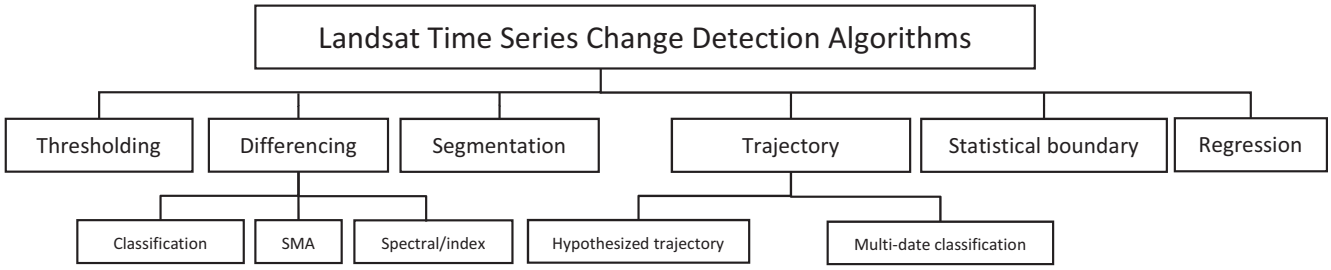

Fig. 4. Categories and subcategories of Landsat time series change detection algorithms.

Table 2
Characteristics of different Landsat time series change detection algorithms.

Category	Subcategory	Temporal Frequency	Change Index	Univariate Multivariate	Online Offline	Abrupt Gradual Both	Subpixel Pixel Spatial	References
Thresholding		Low	Principal Components (PCs)	Multivariate	Offline	Abrupt	Pixel	Hayes and Sader (2001)
		Low	NDVI	Univariate	Offline	Abrupt	Pixel	Lee (2008)
		Medium	NDVI	Univariate	Offline	Abrupt	Pixel	J. Li et al. (2015a)
		Medium	Disturbance index	Univariate	Offline	Abrupt	Pixel	Pickell et al. (2014) and Sieber et al. (2013)
		Medium	Z-scores based on Tasseled Cap Transformation (TCT)	Univariate	Offline	Abrupt	Pixel	Kayastha et al. (2012)
		Medium	Integrated Forest Z-score (IFZ)	Univariate	Offline	Abrupt	Pixel	Chen et al. (2013) and Huang et al. (2010a, 2009)
		High	Multivariate Alteration Detection (MAD) variates	Multivariate	Offline	Abrupt	Pixel	Alaibakhsh et al. (2015)
		High	Disturbance Index (DI), Tasseled Cap Brightness (TCB), Tasseled Cap Wetness (TCW), & normalized NDVI	Multivariate	Offline	Abrupt	Pixel	Hilker et al. (2009)
Differencing	Classification	Low	Land cover	Univariate	Offline	Abrupt	Pixel	Dekker et al. (2005), Giri et al. (2008), Giri and Muhlhausen (2008), Mihai et al. (2015), Muttitanon and Tripathi (2005), Palandro et al. (2003), Pillay et al. (2014), Ramadan et al. (2004), Su (2000), Unger et al. (2015), Yang et al. (2015), Zhang et al. (2013) and Zhao et al. (2014)
		Low	Land cover	Univariate	Offline	Abrupt	Spatial	Liu and Cai (2012)
		Medium	Land cover	Univariate	Offline	Abrupt	Pixel	Palandro et al. (2008)
		High	Land cover	Univariate	Offline	Abrupt	Pixel	Knudby et al. (2010), Kontgis et al. (2015), Li and Narayanan (2003), X. Li et al. (2015), Nutini et al. (2013), Pardo-Pascual et al. (2014), Potapov et al. (2015) and Tulbure and Broich (2013)
	Spectral Mixture Analysis	Low	Impervious fraction	Univariate	Offline	Abrupt	Subpixel	Powell et al. (2008)
		Low	Vegetation and non-vegetation fractions	Multivariate	Offline	Abrupt	Subpixel	Cunningham et al. (2015)
		Medium	Wetland fraction	Univariate	Offline	Abrupt	Subpixel	Dingle Robertson et al. (2015)
	Spectral/ Index	Low	NDVI	Univariate	Offline	Abrupt	Pixel	Hayes and Sader (2001) and Marzen et al. (2011)
		Low	Normalized Difference Wetness Index (NDWI)	Univariate	Offline	Abrupt	Pixel	Jin and Sader (2005)
		Low	Change vector	Multivariate	Offline	Abrupt	Pixel	Fraser et al. (2009) and Vorovencii (2014)
		Medium	Normalized Burn Ratio (NBR)	Univariate	Offline	Abrupt	Pixel	Bolton et al. (2015) and Parker et al. (2015)
		Medium	Chang vector	Multivariate	Offline	Abrupt	Pixel	Zanotta et al. (2015)
		Medium	DI and NBR	Multivariate	Offline	Abrupt	Pixel	Neigh et al. (2014)
		Medium	Enhanced wetness	Univariate	Online	Abrupt	Pixel	Linke et al. (2009)
		High	Red and blue bands	Multivariate	Offline	Abrupt	Pixel	Hagolle et al. (2010)
Segmentation		Medium	NBR	Univariate	Offline	Both	Pixel	Chance et al. (2016), Franklin et al. (2015), Kennedy et al. (2010), Liang et al. (2014), Meigs et al. (2015, 2011) and Senf et al. (2015)
		Medium	NBR	Univariate	Offline	Both	Spatial	Hermosilla et al. (2015a,b) and Kennedy et al. (2015)
		Medium	TCW	Univariate	Offline	Both	Pixel	Frazier et al. (2015), Griffiths et al. (2012) and Grogan et al. (2015)
Trajectory Classification	Hypothesized Trajectory	Low	NDVI & Normalized Difference Water Index (MNDWI)	Multivariate	Offline	Abrupt	Pixel	Xue et al. (2014)
		Low	Tasseled Cap Angle (TCA)	Univariate	Offline	Abrupt	Pixel	Ahmed et al. (2014)
		Low	Short-wave Infrared (SWIR) band	Univariate	Offline	Abrupt	Pixel	Gillanders et al. (2008)
		Medium	SWIR band	Univariate	Offline	Both	Pixel	Kennedy et al. (2007)
	Multi-date Classification	Low	NDVI	Univariate	Offline	Abrupt	Pixel	Hayes and Sader (2001) and Sader et al. (2003)
		Low	NDVI or NDWI	Univariate	Offline	Abrupt	Pixel	Wilson and Sader (2002)
		Low	Spectral bands	Multivariate	Offline	Abrupt	Pixel	Coops et al. (2010) and Gavier-Pizarro et al. (2012)
		Low	Spectral bands	Multivariate	Offline	Abrupt	Spatial	Boucher et al. (2006)
		Low	Normalized Difference Moisture Index (NDMI)	Univariate	Offline	Abrupt	Pixel	Sader and Legaard (2008)
		Medium	Spectral bands	Multivariate	Offline	Abrupt	Pixel	Kaufmann and Seto (2001), Margono et al. (2012) and Sieber et al. (2013)
		Medium	NDVI	Univariate	Offline	Abrupt	Pixel	Maxwell and Sylvester (2012)
		High	Spectral bands metrics	Multivariate	Offline	Abrupt	Pixel	Hansen et al. (2014, 2013) and Potapov et al. (2011, 2012)

Table 2 (*continued*)

Category	Subcategory	Temporal Frequency	Change Index	Univariate Multivariate	Online Offline	Abrupt Gradual Both	Subpixel Pixel Spatial	References
		High	Spectral bands, NDVI, NBR, & NDWI metrics	Multivariate	Online	Abrupt	Pixel	Hansen et al. (2016)
		High	Spectral bands, NDWI, & NDVI metrics	Multivariate	Offline	Abrupt	Pixel	Potapov et al. (2015)
Statistical Boundary		High	Spectral bands	Multivariate	Online	Abrupt	Pixel	Fu and Weng (2016), Goodwin et al. (2013), Goodwin and Collett (2014) and Zhu and Woodcock (2014a,b)
		High	Spectral bands	Multivariate	Online	Both	Pixel	Zhu et al. (2016a)
		High	DI	Univariate	Online	Abrupt	Pixel	Zhu et al. (2012)
		High	NDVI	Univariate	Online	Abrupt	Pixel	Dutrieux et al. (2015)
		High	Fused NDVI and L band scatter	Univariate	Online	Abrupt	Pixel	Reiche et al. (2015)
		High	Spatially normalized NDVI	Univariate	Online	Abrupt	Spatial	Hamunyela et al. (2016)
		High	NDMI	Univariate	Online	Abrupt	Pixel	DeVries et al. (2015)
		High	TCA	Univariate	Online	Both	Pixel	Brooks et al. (2014)
Regression		Low	NDVI, Soil-adjusted Vegetation Index (SAVI), Tasseled Cap Greenness (TCG), or green fraction	Univariate	Offline	Gradual	Pixel, & Subpixel	Sonnenschein et al. (2011)
		Low	TCG or six-band discriminant index	Univariate	Offline	Gradual	Pixel	Lawes and Wallace (2008)
		Medium	Cumulative net change in wetland area	Univariate	Offline	Gradual	Pixel	Fickas et al. (2016)
		Medium	SWIR/NIR ratio	Univariate	Offline	Gradual	Pixel	Vogelmann et al. (2012)
		High	NDVI	Univariate	Online	Both	Pixel	Vogelmann et al. (2016)
		High	NDVI or NDWI	Univariate	Offline	Gradual	Pixel	Latifovic and Pouliot (2014)

process each pixel independently, without considering the spatial domain of the data, but there are some algorithms also consider neighboring pixels (spatial).

4.1. Thresholding

The thresholding method employs a predefined threshold for identifying a land cover (mostly forest) in the time series, and changes are detected when there are significant deviations from the threshold. Usually the Landsat images are transformed to the dimension that is sensitive to a particular cover type. Most of transforms are based on the normalized indices, such as normalized NDVI (Hilker et al., 2009), z-scores based Tasseled Cap Transformation (TCT) (Kayastha et al., 2012), Disturbance Index (DI) (Hilker et al., 2009; Pickell et al., 2014; Sieber et al., 2013), or Integrated Forest Z-score (IFZ) (Chen et al., 2013; Huang et al., 2010a, 2009). NDVI threshold is also used to study changes in vegetation presence (Lee, 2008; J. Li et al., 2015a). Multivariate thresholding methods such as Principal Component Analysis (PCA) (Hayes and Sader, 2001) and Multivariate Alteration Detection (MAD) (Alaibakhsh et al., 2015) have been used to extract the data dimension accounting for the interested change types. Most of the thresholding studies use Landsat time series with medium frequency, and all the thresholding studies used here are offline and only detect abrupt changes at pixel level. The thresholding method is simple to use, but is highly dependent on the threshold that is predefined for a particular cover type.

4.2. Differencing

The differencing method detects change by comparing images acquired at different time, and changes are defined by places that show large differences. Based on the images used for differencing, we can further divide this category into three subcategories: classification, Spectral Mixture Analysis (SMA), and spectral/index. By differencing land cover classification results at different dates, also known as post-classification comparison, changes in land cover will be identified. This method has been widely used in change detection based on Landsat time series, and most of them were based on either low or high frequencies. As each individual image is classified separately, atmospheric correction is unnecessary. Moreover, this method can also provide "from-to" land cover information. However, the accuracy of this method is highly dependent on the accuracy of classification maps, and errors present in each of the map are compounded in the final change map, such that this method is highly vulnerable to classification errors. Methods such as consistency checking or spatial–temporal techniques are reported capable of reducing commission errors in the final change maps derived from classification differencing (X. Li et al., 2015; Liu and Cai, 2012). Similarly, we can compare land cover fractions derived from SMA to detect change for different land cover types (Cunningham et al., 2015; Dingle Robertson et al., 2015; Powell et al., 2008). One benefit of this method is that we can get subpixel information for places that have undergone changes. However, the accuracy of this method is also highly dependent on the accuracy of SMA, and the errors are compounded similarly as the classification differencing method. For the spectral/index method, changes are detected by comparing spectral bands or indices at different time, and all three frequencies of Landsat time series have been used in this subcategory. Change indices such as NDVI (Hayes and Sader, 2001), Normalized Difference Wetness Index (NDWI) (Jin and Sader, 2005), Normalized Burn Ratio (NBR) (Bolton et al., 2015; Neigh et al., 2014; Parker et al., 2015), change vector (Fraser et al., 2009; Vorovencii, 2014), DI (Neigh et al., 2014), enhanced Wetness (Linke et al., 2009), and original spectral bands (Hagolle et al., 2010) have been used in this method. Some of

the studies used a single index (Bolton et al., 2015; Hayes and Sader, 2001; Jin and Sader, 2005; Linke et al., 2009; Marzen et al., 2011; Parker et al., 2015), while others used multiple indices to detect change (Fraser et al., 2009; Hagolle et al., 2010; Neigh et al., 2014; Vorovencii, 2014; Zanotta et al., 2015). The spectral/index method requires accurate radiometric calibration to make the spectral/index comparable between the dates, but as long as the data are well calibrated, the accuracy from this subcategory will be a lot higher than the other two subcategories. All the differencing methods discussed here are offline and only detect abrupt changes. The differencing method is relatively simple to use, but is highly dependent on the consistency of the images to be compared with. Methods of classification and SMA differencing are generally not recommended for change detection due to the likelihood of including compounded errors from classification or SMA.

4.3. Segmentation

The segmentation method is an offline approach that needs to have all the historical time series data available at the same time. By segmenting the time series into a series of straight line segments based on the residual-error and angle criterions, both abrupt and gradual changes can be detected based on the derived straight-line segments at pixel level. Most of the studies in this category are focused on forest change and only use a medium frequency of Landsat time series. NBR (Chance et al., 2016; Franklin et al., 2015; Hermosilla et al., 2015a, 2015b; Kennedy et al., 2015, 2010; Liang et al., 2014; Meigs et al., 2015, 2011; Senf et al., 2015) and Tasseled Cap Wetness (TCW) (Frazier et al., 2015; Griffiths et al., 2012; Grogan et al., 2015) are the only change indices used in this category. Two studies incorporated spatial information to help detect change, in which Kennedy et al. (2015) used spatial adjacency and temporal coherence to improve the final maps, and Hermosilla et al. (2015a,b) relabeled low-reliability changes based on spatially-adjacent high reliability change. The segmentation method is computational expensive, but has shown great potentials in detecting forest change at large scale.

4.4. Trajectory classification

The trajectory classification method first extracts information from Landsat time series for places that have undergone certain kinds of change (for training purpose), and later uses this information to further classify every Landsat time series in the image. Based on how the trajectory of Landsat time series is classified, we can further divide this category into two subcategories: hypothesized trajectory and multi-date classification. For the hypothesized trajectory method, the rules for classifying different kinds of changes are based on the hypothesized trajectories representing signatures specific to different kinds of changes. For the multi-date classification method, there is no hypothesis on the time series trajectories, but rather supervised classifiers are used to classify different change types. In the hypothesized trajectory approach, both low (Ahmed et al., 2014; Gillanders et al., 2008; Xue et al., 2014) and medium (Kennedy et al., 2007) frequencies of Landsat time series have been used. In the multi-date classification method, most of the studies are based on low (Boucher et al., 2006; Coops et al., 2010; Gavier-Pizarro et al., 2012; Hayes and Sader, 2001; Sader et al., 2003; Sader and Legaard, 2008; Wilson and Sader, 2002) and high (Hansen et al., 2016, 2014, 2013; Hansen and Loveland, 2012; Potapov et al., 2011, 2015, 2012) frequencies of Landsat time series, while only a few studies are based on a medium frequency of Landsat time series (Kaufmann and Seto, 2001; Margono et al., 2012; Maxwell and Sylvester, 2012; Sieber et al., 2013). Most of the trajectory classification methods are offline, except Hansen et al. (2016) developed an alerting system that is able to monitor humid tropical forest in near-real time based on newly collected Landsat images. The trajectory classification method is mainly designed to detect abrupt changes, but Kennedy et al. (2007) detected both gradual and abrupt changes based on the hypothesized trajectory method. Moreover, the hypothesized trajectory method favors univariate time series (Ahmed et al., 2014; Gillanders et al., 2008; Kennedy et al., 2007), while the multi-date classification method favors multivariate time series (Boucher et al., 2006; Coops et al., 2010; Gavier-Pizarro et al., 2012; Hansen et al., 2016, 2014, 2013; Kaufmann and Seto, 2001; Margono et al., 2012; Potapov et al., 2012, 2011, 2015; Sieber et al., 2013). The trajectory classification method is computational expensive, and this method requires fully understanding of the characteristics of different kinds of change.

4.5. Statistical boundary

The statistical boundary method expects the time series to follow a statistical boundary and any significant departure from the boundary is detected as a change. All the studies in this category used a high frequency of Landsat time series. Most of the time Landsat time series are decomposed into trend, seasonal change, and noise components before estimating the statistical boundary. Algorithms based on statistical quality control charts (Brooks et al., 2014), econometrics structural change monitoring (DeVries et al., 2015; Dutrieux et al., 2015; Hamunyela et al., 2016; Reiche et al., 2015), and model prediction (Fu and Weng, 2016; Goodwin et al., 2013; Goodwin and Collett, 2014; Vogelmann et al., 2015; Zhu et al., 2016a, 2012; Zhu and Woodcock, 2014a, 2014b) are used for estimating the statistical boundaries. Most of the studies are able to detect change continuously (online), but some of them need to have all the time series available before detecting change (offline) (Goodwin et al., 2013; Goodwin and Collett, 2014; Zhu and Woodcock, 2014b). Univariate time series are widely used, and only a few of them use multiple spectral bands of Landsat time series (Fu and Weng, 2016; Goodwin et al., 2013; Goodwin and Collett, 2014; Zhu et al., 2016a; Zhu and Woodcock, 2014a, 2014b). Most of the studies did not use spatial information to help with change detection, except Hamunyela et al. (2016), which used NDVI values that are spatially normalized (sNDVI) based on different window sizes to reduce phenological differences. They suggested that by integrating this spatial information, change can be identified with less delay. Most of the algorithms in this category have the potential of detecting both gradual and abrupt changes, but only Brooks et al. (2014) and Zhu et al. (2016a) demonstrated this capability. The statistical boundary method is very computational expensive and requires large storage. However, this method can detect change much faster and is usually less influenced by the seasonal differences.

4.6. Regression

The regression method assumes there is a linear relationship between predictor and response variables and uses regression to get the answer. The predictor variables are usually the time of the observations, and the response variables are usually the observed values (spectral bands or indices). The main purpose of the regression method is to estimate the long-term movements or trends in time series, which are mostly gradual changes. All regression studies are univariate and changes are detected in an offline manner. Variables such as NDVI, NDWI, Soil-adjusted Vegetation Index (SAVI), TCT components, green vegetation fraction, six-band discriminant index, Short-wave Infrared (SWIR)/NIR ratio, are used as change indices. Most of the studies use pixel as the smallest unit, except Sonnenschein et al. (2011) used green vegeta-

tion fraction as the predictor variable (sub-pixel scale). The regression method is heavily reliant on the accurate calibration of different Landsat sensors. Landsat sensors including MSS, TM, and ETM+ have been placed onto a consistent radiometric scale (Markham and Helder, 2012). However, the OLI data are reported to have some differences when compared with previous Landsat sensors (Holden and Woodcock, 2016; Roy et al., 2016; Zhu et al., 2016a). Moreover, Zhang and Roy (2016) found there are some inconsistencies in the Landsat 5 NDVI time series caused by satellite orbit change, while Sulla-Menashe et al. (2016) suggested that the red reflectance from Landsat 7 is lower than that from Landsat 5, which introduces artificial long-term trends in NDVI. All frequencies (low, medium, and high) have been used in the regression method. For low and medium frequencies, seasonal changes are the main sources of noise in trend analysis, such that images from near-anniversary date and within growing season are preferred. Normally, the regression method assumes there is no abrupt change in the time series, except Vogelmann et al. (2016) considered the possibility of both gradual and abrupt changes in Landsat time series. The regression method is relatively simple to use, but it is mostly designed to quantify long-term trends in the time series, and is less ideal for detecting changes that are abrupt in the Landsat time series. Moreover, as the regression method is highly dependent on the consistency of different sensors, it is important to calibrate all sensors to make sure the significant trends are statistically meaningful.

4.7. Some of the widely-used algorithms

Table 3 lists some of the widely-used change detection algorithms that use Landsat time series as their inputs. The Landsat-based detection of Trends in Disturbance and Recovery (LandTrendr; Kennedy et al., 2010) algorithm uses the segmentation method to detect abrupt change (forest disturbance) and, between the abrupt changes, a slope is fitted for each segment to capture the gradual changes (forest recovery in this study). The LandTrendr algorithm is an offline and univariate approach that uses NBR as its main change index. This algorithm has been used for many applications, such as attribution of disturbance change agents (Kennedy et al., 2015), insect infestation detection (Liang et al., 2014; Meigs et al., 2015, 2011; Senf et al., 2015), forest change detection (Griffiths et al., 2012; Grogan et al., 2015; Kennedy et al., 2012, 2010), and land cover change detection (Franklin et al., 2015). The Vegetation Change Tracker (VCT; Huang et al., 2010a) algorithm normalizes each Landsat image into a forest probability index called integrated forest z-score and uses the thresholding method to detect forest disturbance. The VCT algorithm is an offline and univariate method. It is mainly focused on detecting abrupt changes in vegetation, such as forest disturbance (Chen et al., 2013; Huang et al., 2010a, 2009; Pickell et al., 2014) and wetland change (Kayastha et al., 2012). Both the LandTrendr and VCT algorithms use a medium frequency of Landsat time series, and are capable of providing change information on an annual timescale. The Breaks for Additive Season and Trend (BFAST) algorithm belongs to the statistical boundary method, and it was rooted in the econometrics discipline for monitoring structural change (Chu et al., 1995; Leisch et al., 2000; Zeileis et al., 2005). The BFAST algorithm decomposes time series into trend, season, and noise components, which makes it possible to detect abrupt change as well as gradual change. This algorithm was originally developed for detecting vegetation change in 16-day MODIS composite time series in an offline mode (Verbesselt et al., 2010), and was later modified and renamed (BFAST Monitor) to detect drought-related vegetation disturbance in near real-time using MODIS time series (online) (Verbesselt et al., 2012). Recently, the BFAST Monitor algorithm has been applied to Landsat time series for detecting forest change (DeVries et al., 2015; Dutrieux et al., 2015; Hamunyela et al., 2016; Reiche et al., 2015). The BFAST Monitor algorithm uses a high frequency of Landsat time series, and is a univariate (e.g., NDVI most of the time) approach. The Continuous Change Detection and Classification (CCDC; Zhu and Woodcock, 2014a) algorithm is a statistical boundary method that uses all available Landsat data (high frequency). It is evolved from a Continuous Monitoring of Forest Disturbance Algorithm (CMFDA), which is designed to detect forest disturbance (abrupt changes) based on all available Landsat data (Zhu et al., 2012). The CCDC algorithm has expanded the change target from forest to many land cover types and added a slope component to detect gradual changes. To detect many kinds of surface change, all spectral bands (multivariate) were used to define a change; the "continuous" character makes CCDC capable of detecting change as soon as new Landsat images are collected (online). The CCDC algorithm has been used to study abrupt changes such as land cover change (Fu and Weng, 2016; Zhu and Woodcock, 2014a), as well as gradual vegetation changes (Vogelmann et al., 2015; Zhu et al., 2016a). Recently, Zhu et al. (2015b) made several major updates to improve its change detection results, and Zhu et al. (2016b) optimized the strategy for selecting training and auxiliary data for improving classification results. Currently, the CCDC algorithm has been chosen as the change detection algorithm for the USGS Land Change Monitoring, Assessment, and Projection (LCMAP) program for generating land change products for the United States (Pengra et al., 2016; Zhu et al., 2016b). Hansen et al. (2013) produced the first global map of annual forest change based on a high frequency of Landsat time series using the multi-date classification method. This approach uses multiple Landsat spectral bands (multivariate) and is an offline algorithm. Similar approaches have been applied to other parts of the world, mainly for detecting forest change (Hansen et al., 2014; Margono et al., 2012; Potapov et al., 2015, 2012), and recently it has been modified to an online approach for disturbance alerts in humid tropical forest (Hansen et al., 2016). One common character of these widely-used algorithms is that all of these algorithms are fully automated and are

Table 3
Characteristics of some of the widely-used algorithms.

Algorithm Name	Temporal Frequency	Change Index	Univariate Multivariate	Online Offline	Abrupt gradual	Sub-pixel Pixel spatial	Applications	References
LandTrendr	Medium	NBR	Univariate	Offline	Both	Pixel	Forest disturbance and recovery	Kennedy et al. (2010)
VCT	Medium	IFZ	Univariate	Offline	Abrupt	Pixel	Forest disturbance	Huang et al. (2010a)
BFAST monitor	High	NDVI	Univariate	Online	Both	Pixel	Drought-related vegetation disturbance	Verbesselt et al. (2012)
CCDC	High	Spectral bands	Multivariate	Online	Both	Pixel	Land cover change	Zhu and Woodcock (2014a)
NA	High	Spectral bands	Multivariate	Offline	Both	Pixel	Forest gain and loss	Hansen et al. (2013)

capable of detecting change at large scale (from regional to global) and within a short time period (from annual to weekly). The other common character is that many of these algorithms (i.e., LandTrendr, BFAST, and CCDC) are publicly available, which further popularized the use of these algorithms.

5. Applications

Change detection based on Landsat time series has many applications. Generally, we can divide these applications into two categories: change target and change agent detection.

5.1. Change target

Knowing what is changing – the "change target" – is important in change detection. By limiting changes detected within the targeted land cover and use types, change can be better detected based on thresholds and change indices that are determined and selected specifically for the change target.

The change target is usually quite broad, which involves changes in a variety of land cover and land use classes. Classification differencing is the most widely used method (Liu and Cai, 2012; Muttitanon and Tripathi, 2005; Nutini et al., 2013; Pillay et al., 2014; Zhang et al., 2013; Zhao et al., 2014). There are also methods based on spectral/index differencing (Fraser et al., 2009; Linke et al., 2009; Vorovencii, 2014), trajectory classification (Boucher et al., 2006; Gillanders et al., 2008; Kaufmann and Seto, 2001; Sieber et al., 2013), segmentation (Franklin et al., 2015), and statistical boundary (Fu and Weng, 2016; Zhu and Woodcock, 2014a).

Some change detection studies have focused on only one land cover type. The most studies target has been forest, in which the methods of statistical boundary (Brooks et al., 2014; Dutrieux et al., 2015; Hamunyela et al., 2016; Reiche et al., 2015; Zhu et al., 2012), thresholding (Chen et al., 2013; Hilker et al., 2009; Huang et al., 2010a, 2009; Lee, 2008), multi-date classification (Hansen et al., 2016, 2014; Margono et al., 2012; Potapov et al., 2015, 2012; Sader and Legaard, 2008; Wilson and Sader, 2002), differencing (Bolton et al., 2015; Hayes and Sader, 2001; Jin and Sader, 2005; Zanotta et al., 2015), segmentation (Chance et al., 2016; DeVries et al., 2015; Frazier et al., 2015; Griffiths et al., 2012; Grogan et al., 2015; Hermosilla et al., 2015a; Kennedy et al., 2012, 2010), and trajectory classification (Ahmed et al., 2014; Sader et al., 2003) have been used. There are also change detection studies that are mainly focusing on studying the long-term trends of vegetation using the regression method (Latifovic and Pouliot, 2014; Sonnenschein et al., 2011; Vogelmann et al., 2012). Cloud can be detected based on the statistical boundary change detection method (Goodwin et al., 2013; Zhu and Woodcock, 2014b). Wetland change can be detected based on regression (Fickas et al., 2016), thresholding (Kayastha et al., 2012), and SMA differencing (Dingle Robertson et al., 2015). There are also studies focused on changes in coral reefs (Palandro et al., 2003, 2008), water (Li and Narayanan, 2003; Tulbure and Broich, 2013), seagrass (Dekker et al., 2005), and mangrove (Giri et al., 2008; Giri and Muhlhausen, 2008) based on the classification differencing method. Note that by focusing on one or a few change targets, the identified changes are usually related to the categorical changes for these change targets. If a change event occurred to the change target but did not change the type of the cover (for example, forest impacted by beetle infestation is still a forest pixel), this change will not be identified in this kind of application. Moreover, there is a growing trend that many more studies are focusing on a single change target instead of many land cover/use type, due to the benefit of choosing more precise thresholds and better change indices for the interested change target.

5.2. Change agent

Understanding the cause of change – the "change agent" – is also valuable in change detection. For natural changes, the agent refers to different kinds of natural events, such as fire, insect infestation, storm, flooding, and drought. For anthropogenic changes, the agent refers to the human induced change (mostly land use related), such as urban development, farming, logging, and mining.

Most of the change agent studies have only focused on a single change agent, such as urban development, farming, insect infestation, fire, logging, mining, storm, and petroleum exploration/production. For urban development, classification differencing is the main method used to identify urban related changes (X. Li et al., 2015; Mihai et al., 2015; Ramadan et al., 2004). SMA differencing can also be used to quantify impervious surface change (Cunningham et al., 2015; Powell et al., 2008). Hypothesized trajectory is another approach for detecting urban growth (Xue et al., 2014). For farming related changes, Kontgis et al. (2015) used classification differencing to map rice paddy extent and intensification, and Maxwell and Sylvester (2012) used multi-date classification to map "ever-cropped" land. For insect infestation related change, segmentation methods, such as LandTrendr have been widely used (Liang et al., 2014; Meigs et al., 2015, 2011; Senf et al., 2015). Coops et al. (2010) also tested using multi-date classification method to detect forest changes following insect infestation. For fire related changes, Parker et al. (2015) used spectral/index differencing and mapped fire severity based on differences in NBR, and Goodwin and Collett (2014) proposed a statistical boundary method for mapping fire history. For forest logging/harvest related change, the multi-date classification approach is the most common method used (Schroeder et al., 2012; Wilson and Sader, 2002). For mining related changes, J. Li et al. (2015a) used the thresholding method to reconstruct mining activity and Gillanders et al. (2008) explored mining impacts on land cover change based on the hypothesized trajectory method. For storm related changes, Pardo-Pascual et al. (2014) used the classification differencing method to evaluate the impact of storm on sandy beaches. Unger et al. (2015) studied the impacts of petroleum exploration and production on land cover based on the classification differencing method.

Some of the studies can also detect and classify multiple change agents. Neigh et al. (2014) detected all forest changes based on spectral/index differencing and then used supervised classification to separate different kinds of change agents, including logging, fire, and insect. Kennedy et al. (2015) used segmentation method (Landtrendr) to detect changes in NBR time series and then used topographic data, change related information, and patch shape index to classify many change agents, including agriculture, forest management, natural change, and riparian. Alaibakhsh et al. (2015) used the thresholding method (MAD); change agents, such as climate variability, fire events, and mining activity were detected based on each of the six MAD variates. Note that by detecting change based on its agent, we will be able to detect change even if the land cover/use type is still the same before and after the change event. However, for this application, we need to have good understanding of the different change agents within the study area. Moreover, for a long time, many algorithms were only designed to detect a single change agent, but algorithms with the capability of detecting multiple change agents are attracting more and more attentions.

6. Conclusions

The free and open Landsat data distribution policy started in 2008 has completely revolutionized the way of utilizing Landsat

data and has stimulated many novel change detection algorithms based on Landsat time series. We have endeavored to keep updated with all the newly published studies involving the use of Landsat time series for change detection, but there are always new algorithms and applications coming out, even during the process of writing this review. Among all the studies, a general trend is observed: the more recent the study, the higher the frequency of the Landsat time series used. At the same time, automated image preprocessing algorithms like LEDAPS and Fmask are being widely used, which further facilitate the use of Landsat time series. Based on the mathematical methods used for detecting change, we divide all change detection algorithms into six categories, including thresholding, differencing, segmentation, trajectory classification, statistical boundary, and regression. Each category has its own limitations and strengths, and users should understand each method well before conducing change detection with Landsat time series.

Currently, most of the time series algorithms are heavily focused on the temporal domain of the Landsat data, and the spatial domain of the data is almost entirely neglected. More algorithms that use the spatial–temporal techniques are anticipated. Though many online change detection algorithms have been developed, most of the change detection products derived from Landsat time series are at least one years old, which are not management relevant. More near real-time change detection products derived from Landsat time series are expected. The change detection applications of the Landsat time series cover a wide range of topics, however, at present, most of the applications are limited to small areas due to constraints of storage and computing resources. With the advances in high-performance computing and cheaper storage, applications based on Landsat time series at continental or even global scale will be the mainstream in the next a few years.

Acknowledgements

We gratefully acknowledge the USGS leadership in the data policy that facilitated the advances in Landsat time series analysis. This research was supported by USGS Great Plains Cooperative Ecosystem Studies Unit (CESU) Program (grant number G17AC00057).

References

Ackerman, S.A., Strabala, K.I., Menzel, W.P., Frey, R.a., Moeller, C.C., Gumley, L.E., 1998. Discriminating clear sky from clouds with MODIS. J. Geophys. Res. 103, 32141–32157. http://dx.doi.org/10.1029/1998JD200032.

Ahmed, O.S., Franklin, S.E., Wulder, M.A., 2014. Interpretation of forest disturbance using a time series of Landsat imagery and canopy structure from airborne lidar. Can. J. Remote Sens. 39, 521–542. http://dx.doi.org/10.5589/M14-004.

Alaibakhsh, M., Emelyanova, I., Barron, O., Khiadani, M., 2015. Multivariate detection and attribution of land-cover changes in the Central Pilbara, Western Australia. Int. J. Remote. http://dx.doi.org/10.1080/01431161.2015.1042595.

Banskota, A., Kayastha, N., Falkowski, M.J., Wulder, M.A., Froese, R.E., White, J.C., 2014. Forest monitoring using landsat time series data: a review. Can. J. Remote Sens. 40, 362–384. http://dx.doi.org/10.1080/07038992.2014.987376.

Berk, A., Bernstein, L.S., Anderson, G.P., Acharya, P.K., Robertson, D.C., Chetwynd, J. H., 1998. MODTRAN Cloud and Multiple Scattering Upgrades with Application to AVIRIS 4257.

Bolton, D.K., Coops, N.C., Wulder, M.A., 2015. Characterizing residual structure and forest recovery following high-severity fire in the western boreal of Canada using Landsat time-series and airborne lidar data. Remote Sens. Environ. 163, 48–60. http://dx.doi.org/10.1016/j.rse.2015.03.004.

Boriah, S., 2010. Time series change detection: Algorithms for land cover change 160.

Boucher, a., Seto, K.C., Journel, a.G., 2006. A novel method for mapping land cover changes: incorporating time and space with geostatistics. IEEE Trans. Geosci. Remote Sens. 44, 3427–3435. http://dx.doi.org/10.1109/TGRS.2006.879113.

Braaten, J.D., Cohen, W.B., Yang, Z., 2015. Automated cloud and cloud shadow identification in Landsat MSS imagery for temperate ecosystems. Remote Sens. Environ. 169, 128–138. http://dx.doi.org/10.1016/j.rse.2015.08.006.

Brooks, E.B., Wynne, R.H., Thomas, V.A., Blinn, C.E., Coulston, J.W., 2014. On-the-fly massively multitemporal change detection using statistical quality control charts and landsat data. IEEE Trans. Geosci. Remote Sens. 52, 3316–3332. http://dx.doi.org/10.1109/TGRS.2013.2272545.

Chance, C.M., Hermosilla, T., Coops, N.C., Wulder, M.A., White, J.C., 2016. Effect of topographic correction on forest change detection using spectral trend analysis of Landsat pixel-based composites. Int. J. Appl. Earth Obs. Geoinf. 44, 186–194. http://dx.doi.org/10.1016/j.jag.2015.09.003.

Chávez, P.S.J., 1996. Image-based atmospheric corrections - revisited and improved. Photogramm. Eng. Remote Sensing 62, 1025–1036. doi: 0099-1112/96/6209-1025.

Chen, X., Vogelmann, J.E., Chander, G., Ji, L., Tolk, B., Huang, C., Rollins, M., 2013. Cross-sensor comparisons between Landsat 5 TM and IRS-P6 AWiFS and disturbance detection using integrated Landsat and AWiFS time-series images. Int. J. Remote Sens. 34, 2432–2453. http://dx.doi.org/10.1080/01431161.2012.743690.

Chu, C., shang, J., Hornik, K., Kaun, C.M., 1995. Mosum tests for parameter constancy. Biometrika 82, 603–617. http://dx.doi.org/10.1093/biomet/82.3.603.

Coops, N.C., Gillanders, S.N., Wulder, M.A., Gergel, S.E., Nelson, T., Goodwin, N.R., 2010. Assessing changes in forest fragmentation following infestation using time series Landsat imagery. For. Ecol. Manage. 259, 2355–2365. http://dx.doi.org/10.1016/j.foreco.2010.03.008.

Coppin, P., Jonckheere, I., Nackaerts, K., Muys, B., Lambin, E., 2004. Review ArticleDigital change detection methods in ecosystem monitoring: a review. Int. J. Remote Sens. 25, 1565–1596. http://dx.doi.org/10.1080/0143116031000101675.

Cunningham, S., Rogan, J., Martin, D., DeLauer, V., McCauley, S., Shatz, A., 2015. Mapping land development through periods of economic bubble and bust in Massachusetts using Landsat time series data. GIScience Remote Sens. 1603. http://dx.doi.org/10.1080/15481603.2015.1045277.

Dekker, A.G., Brando, V.E., Anstee, J.M., 2005. Retrospective seagrass change detection in a shallow coastal tidal Australian lake. Remote Sens. Environ. 97, 415–433. http://dx.doi.org/10.1016/j.rse.2005.02.017.

Derrien, M., Farki, B., Harang, L., LeGléau, H., Noyalet, A., Pochic, D., Sairouni, A., 1993. Automatic cloud detection applied to NOAA-11 /AVHRR imagery. Remote Sens. Environ. 46, 246–267. http://dx.doi.org/10.1016/0034-4257(93)90046-Z.

DeVries, B., Decuyper, M., Verbesselt, J., Zeileis, A., Herold, M., Joseph, S., 2015. Tracking disturbance-regrowth dynamics in tropical forests using structural change detection and Landsat time series. Remote Sens. Environ. 169, 320–334. http://dx.doi.org/10.1016/j.rse.2015.08.020.

Dingle Robertson, L., King, D.J., Davies, C., 2015. Assessing land cover change and anthropogenic disturbance in wetlands using vegetation fractions derived from landsat 5 TM imagery (1984–2010). Wetlands 35, 1077–1091. http://dx.doi.org/10.1007/s13157-015-0696-5.

Dutrieux, L.P., Verbesselt, J., Kooistra, L., Herold, M., 2015. Monitoring forest cover loss using multiple data streams, a case study of a tropical dry forest in Bolivia. ISPRS J. Photogramm. Remote Sens. 107, 112–125. http://dx.doi.org/10.1016/j.isprsjprs.2015.03.015.

Fickas, K.C., Cohen, W.B., Yang, Z., 2016. Landsat-based monitoring of annual wetland change in the Willamette Valley of Oregon, USA from 1972 to 2012. Wetl. Ecol. Manage. 24, 73–92. http://dx.doi.org/10.1007/s11273-015-9452-0.

Franklin, S.E., Ahmed, O.S., Wulder, M.A., White, J.C., Hermosilla, T., Coops, N.C., 2015. Large area mapping of annual land cover dynamics using multitemporal change detection and classification of landsat time series data. Can. J. Remote Sens. 41, 293–314. http://dx.doi.org/10.1080/07038992.2015.1089401.

Fraser, R.H., Olthof, I., Pouliot, D., 2009. Monitoring land cover change and ecological integrity in Canada's national parks. Remote Sens. Environ. 113, 1397–1409. http://dx.doi.org/10.1016/j.rse.2008.06.019.

Frazier, R.J., Coops, N.C., Wulder, M.A., 2015. Boreal Shield forest disturbance and recovery trends using Landsat time series. Remote Sens. Environ. 170, 317–327. http://dx.doi.org/10.1016/j.rse.2015.09.015.

Fu, P., Weng, Q., 2016. A time series analysis of urbanization induced land use and land cover change and its impact on land surface temperature with Landsat imagery. Remote Sens. Environ. 175, 205–214. http://dx.doi.org/10.1016/j.rse.2015.12.040.

Gao, F., Hilker, T., Zhu, X., Anderson, M., Masek, J., Wang, P., Yang, Y., 2015. Fusing landsat and MODIS data for vegetation monitoring. IEEE Geosci. Remote Sens. Mag. 3, 47–60. http://dx.doi.org/10.1109/MGRS.2015.2434351.

Gao, F., Masek, J., Schwaller, M., Hall, F., 2006. On the blending of the landsat and MODIS surface reflectance: Predicting daily landsat surface reflectance. IEEE Trans. Geosci. Remote Sens. 44, 2207–2218. http://dx.doi.org/10.1109/TGRS.2006.872081.

Gavier-Pizarro, G.I., Kuemmerle, T., Hoyos, L.E., Stewart, S.I., Huebner, C.D., Keuler, N.S., Radeloff, V.C., 2012. Monitoring the invasion of an exotic tree (Ligustrum lucidum) from 1983 to 2006 with Landsat TM/ETM + satellite data and Support Vector Machines in Córdoba, Argentina. Remote Sens. Environ. 122, 134–145. http://dx.doi.org/10.1016/j.rse.2011.09.023.

Gillanders, S.N., Coops, N.C., Wulder, M.A., Goodwin, N.R., 2008. Application of Landsat satellite imagery to monitor land-cover changes at the Athabasca Oil Sands, Alberta, Canada. Can. Geogr. 52, 466–485. http://dx.doi.org/10.1111/j.1541-0064.2008.00225.x.

Giri, C., Muhlhausen, J., 2008. Mangrove forest distributions and dynamics in Madagascar (1975–2005). Sensors 8, 2104–2117. http://dx.doi.org/10.3390/s8042104.

Giri, C., Zhu, Z., Tieszen, L.L., Singh, A., Gillette, S., Kelmelis, J.A., 2008. Mangrove forest distributions and dynamics (19752005) of the tsunami-affected region of Asia. J. Biogeogr. 35, 519–528. http://dx.doi.org/10.1111/j.1365-2699.2007.01806.x.

Goodwin, N.R., Collett, L.J., 2014. Development of an automated method for mapping fire history captured in Landsat TM and ETM + time series across Queensland, Australia. Remote Sens. Environ. 148, 206–221. http://dx.doi.org/10.1016/j.rse.2014.03.021.

Goodwin, N.R., Collett, L.J., Denham, R.J., Flood, N., Tindall, D., 2013. Cloud and cloud shadow screening across Queensland, Australia: An automated method for Landsat TM/ETM + time series. Remote Sens. Environ. 134, 50–65. http://dx.doi.org/10.1016/j.rse.2013.02.019.

Griffiths, P., Kuemmerle, T., Kennedy, R.E., Abrudan, I.V., Knorn, J., Hostert, P., 2012. Using annual time-series of Landsat images to assess the effects of forest restitution in post-socialist Romania. Remote Sens. Environ. 118, 199–214. http://dx.doi.org/10.1016/j.rse.2011.11.006.

Griffiths, P., van der Linden, S., Kuemmerle, T., Hostert, P., 2013. A pixel-based landsat compositing algorithm for large area land cover mapping. Sel. Top. Appl. Earth Obs. Remote Sensing, IEEE J. 6, 2088–2101. http://dx.doi.org/10.1109/JSTARS.2012.2228167.

Grogan, K., Pflugmacher, D., Hostert, P., Kennedy, R., Fensholt, R., 2015. Cross-border forest disturbance and the role of natural rubber in mainland Southeast Asia using annual Landsat time series. Remote Sens. Environ. 169, 438–453. http://dx.doi.org/10.1016/j.rse.2015.03.001.

Hagolle, O., Huc, M., Pascual, D.V., Dedieu, G., 2010. A multi-temporal method for cloud detection, applied to FORMOSAT-2, VENμS, LANDSAT and SENTINEL-2 images. Remote Sens. Environ. 114, 1747–1755. http://dx.doi.org/10.1016/j.rse.2010.03.002.

Hamunyela, E., Verbesselt, J., Herold, M., 2016. Using spatial context to improve early detection of deforestation from Landsat time series. Remote Sens. Environ. 172, 126–138. http://dx.doi.org/10.1016/j.rse.2015.11.006.

Hansen, M.C., Egorov, A., Potapov, P.V., Stehman, S.V., Tyukavina, A., Turubanova, S. A., Roy, D.P., Goetz, S.J., Loveland, T.R., Ju, J., Kommareddy, A., Kovalskyy, V., Forsyth, C., Bents, T., 2014. Monitoring conterminous United States (CONUS) land cover change with Web-Enabled Landsat Data (WELD). Remote Sens. Environ. 140, 466–484. http://dx.doi.org/10.1016/j.rse.2013.08.014.

Hansen, M.C., Krylov, A., Tyukavina, A., Potapov, P.V., Turubanova, S., Zutta, B., Ifo, S., Margono, B., Stolle, F., Moore, R., 2016. Humid tropical forest disturbance alerts using Landsat data. Environ. Res. Lett. 11, 34008. http://dx.doi.org/10.1088/1748-9326/11/3/034008.

Hansen, M.C., Loveland, T.R., 2012. A review of large area monitoring of land cover change using Landsat data. Remote Sens. Environ. 122, 66–74. http://dx.doi.org/10.1016/j.rse.2011.08.024.

Hansen, M.C.C., Potapov, P.V., Moore, R., Hancher, M., Turubanova, S.A.a., Tyukavina, A., Thau, D., Stehman, S.V.V., Goetz, S.J.J., Loveland, T.R.R., Kommareddy, a., Egorov, A., Chini, L., Justice, C.O.O., Townshend, J.R.G.R.G., Patapov, P.V., Moore, R., Hancher, M., Turubanova, S.A.a., Tyukavina, A., Thau, D., Stehman, S.V.V., Goetz, S.J.J., Loveland, T.R.R., Kommaredy, A., Egorov, A., Chini, L., Justice, C.O.O., Townshend, J.R.G.R.G., 2013. High-Resolution Global Maps of. Science (80-) 342, 850–854. http://dx.doi.org/10.1126/science.1244693.

Hayes, D.J., Sader, S.a., 2001. Comparison of change detection techniques for monitoring tropical forest clearing and vegetation regrowth in a time series. Photogramm. Eng. Remote Sens. 67 (9), 1067–1075. doi:citeulike-article-id:7954186.

Hermosilla, T., Wulder, M.A., White, J.C., Coops, N.C., Hobart, G.W., 2015a. Regional detection, characterization, and attribution of annual forest change from 1984 to 2012 using Landsat-derived time-series metrics. Remote Sens. Environ. 170, 121–132. http://dx.doi.org/10.1016/j.rse.2015.09.004.

Hermosilla, T., Wulder, M.A., White, J.C., Coops, N.C., Hobart, G.W., 2015b. An integrated Landsat time series protocol for change detection and generation of annual gap-free surface reflectance composites. Remote Sens. Environ. 158, 220–234. http://dx.doi.org/10.1016/j.rse.2014.11.005.

Hilker, T., Wulder, M.A., Coops, N.C., Linke, J., McDermid, G., Masek, J.G., Gao, F., White, J.C., 2009. A new data fusion model for high spatial- and temporal-resolution mapping of forest disturbance based on Landsat and MODIS. Remote Sens. Environ. 113, 1613–1627. http://dx.doi.org/10.1016/j.rse.2009.03.007.

Holben, B.N., 1986. Characteristics of maximum-value composite images from temporal AVHRR data. Int. J. Remote Sens. 7, 1417–1434. http://dx.doi.org/10.1080/01431168608948945.

Holden, C.E., Woodcock, C.E., 2016. An analysis of Landsat 7 and Landsat 8 underflight data and the implications for time series investigations. Remote Sens. Environ. 185, 16–36. http://dx.doi.org/10.1016/j.rse.2016.02.052.

Huang, C., Goward, S.N., Masek, J.G., Thomas, N., Zhu, Z., Vogelmann, J.E., 2010a. An automated approach for reconstructing recent forest disturbance history using dense Landsat time series stacks. Remote Sens. Environ. 114, 183–198. http://dx.doi.org/10.1016/j.rse.2009.08.017.

Huang, C., Goward, S.N., Schleeweis, K., Thomas, N., Masek, J.G., Zhu, Z., 2009. Dynamics of national forests assessed using the Landsat record: Case studies in eastern United States. Remote Sens. Environ. 113, 1430–1442. http://dx.doi.org/10.1016/j.rse.2008.06.016.

Huang, C., Thomas, N., Goward, S.N., Masek, J.G., Zhu, Z., Townshend, J.R.G., Vogelmann, J.E., 2010b. Automated masking of cloud and cloud shadow for forest change analysis using Landsat images. Int. J. Remote Sens. 31, 5449–5464. http://dx.doi.org/10.1080/01431160903369642.

Hughes, M.J., Hayes, D.J., 2014. Automated detection of cloud and cloud shadow in single-date Landsat imagery using neural networks and spatial post-processing. Remote Sens. 6, 4907–4926. http://dx.doi.org/10.3390/rs6064907.

Irish, R.R., 2000. Landsat 7 automatic cloud cover assessment. AeroSense 2000 (4049), 348–355. http://dx.doi.org/10.1117/12.410358.

Irish, R.R., Barker, J.L., Goward, S.N., Arvidson, T., 2006. Characterization of the Landsat-7 ETM + Automated Cloud-Cover Assessment (ACCA) Algorithm. Photogramm. Eng. Remote Sens. 72, 1179–1188. http://dx.doi.org/10.14358/PERS.72.10.1179.

Jin, S., Homer, C., Yang, L., Xian, G., Fry, J., Danielson, P., Townsend, P.a., 2013. Automated cloud and shadow detection and filling using two-date Landsat imagery in the USA. Int. J. Remote Sens. 34, 1540–1560. http://dx.doi.org/10.1080/01431161.2012.720045.

Jin, S., Sader, S.A., 2005. Comparison of time series tasseled cap wetness and the normalized difference moisture index in detecting forest disturbances. Remote Sens. Environ. 94, 364–372. http://dx.doi.org/10.1016/j.rse.2004.10.012.

Kaufmann, R.K., Seto, K.C., 2001. Change detection, accuracy, and bias in a sequential analysis of Landsat imagery in the Pearl River Delta, China: Econometric techniques. Agric. Ecosyst. Environ. 85, 95–105. http://dx.doi.org/10.1016/S0167-8809(01)00190-6.

Kayastha, N., Thomas, V., Galbraith, J., Banskota, A., 2012. Monitoring wetland change using inter-annual landsat time-series data. Wetlands 32, 1149–1162. http://dx.doi.org/10.1007/s13157-012-0345-1.

Kennedy, R.E., Andréfouët, S., Cohen, W.B., Gómez, C., Griffiths, P., Hais, M., Healey, S.P., Helmer, E.H., Hostert, P., Lyons, M.B., Meigs, G.W., Pflugmacher, D., Phinn, S. R., Powell, S.L., Scarth, P., Sen, S., Schroeder, T.A., Schneider, A., Sonnenschein, R., Vogelmann, J.E., Wulder, M.A., Zhu, Z., 2014. Bringing an ecological view of change to landsat-based remote sensing. Front. Ecol. Environ. 12, 339–346. http://dx.doi.org/10.1890/130066.

Kennedy, R.E., Cohen, W.B., Schroeder, T.A., 2007. Trajectory-based change detection for automated characterization of forest disturbance dynamics. Remote Sens. Environ. 110, 370–386. http://dx.doi.org/10.1016/j.rse.2007.03.010.

Kennedy, R.E., Yang, Z., Braaten, J., Copass, C., Antonova, N., Jordan, C., Nelson, P., 2015. Attribution of disturbance change agent from Landsat time-series in support of habitat monitoring in the Puget Sound region, USA. Remote Sens. Environ. 166, 271–285. http://dx.doi.org/10.1016/j.rse.2015.05.005.

Kennedy, R.E., Yang, Z., Cohen, W.B., 2010. Detecting trends in forest disturbance and recovery using yearly Landsat time series: 1. LandTrendr - Temporal segmentation algorithms. Remote Sens. Environ. 114, 2897–2910. http://dx.doi.org/10.1016/j.rse.2010.07.008.

Kennedy, R.E., Yang, Z., Cohen, W.B., Pfaff, E., Braaten, J., Nelson, P., 2012. Spatial and temporal patterns of forest disturbance and regrowth within the area of the Northwest Forest Plan. Remote Sens. Environ. 122, 117–133. http://dx.doi.org/10.1016/j.rse.2011.09.024.

Knudby, A., Newman, C., Shaghude, Y., Muhando, C., 2010. Simple and effective monitoring of historic changes in nearshore environments using the free archive of Landsat imagery. Int. J. Appl. Earth Obs. Geoinf. 12, 116–122. http://dx.doi.org/10.1016/j.jag.2009.09.002.

Kontgis, C., Schneider, A., Ozdogan, M., 2015. Mapping rice paddy extent and intensification in the Vietnamese Mekong River Delta with dense time stacks of Landsat data. Remote Sens. Environ. 169, 255–269. http://dx.doi.org/10.1016/j.rse.2015.08.004.

Latifovic, R., Pouliot, D., 2014. Monitoring cumulative long-term vegetation changes over the Athabasca Oil Sands region. IEEE J. Sel. Top. Appl. Earth Obs. Remote Sens. 7, 3380–3392. http://dx.doi.org/10.1109/JSTARS.2014.2321058.

Lawes, R.A., Wallace, J.F., 2008. Monitoring an invasive perennial at the landscape scale with remote sensing. Ecol. Manage. Restor. 9, 53–59. http://dx.doi.org/10.1111/j.1442-8903.2008.00387.x.

Lee, H., 2008. Mapping deforestation and age of evergreen trees by applying a binary coding method to time-series landsat november images. IEEE Trans. Geosci. Remote Sens. 46, 3926–3936. http://dx.doi.org/10.1109/TGRS.2008.2001158.

Leisch, F., Hornik, K., Kuan, C.-M., 2000. Monitoring structural changes with the generalized fluctuation test. Econom. Theory 16, 835–854. doi:null.

Li, J., Narayanan, R.M., 2003. A shape-based approach to change detection of lakes using time series remote sensing images. Geosci. Remote Sensing, IEEE Trans. 41, 2466–2477.

Li, J., Zipper, C.E., Donovan, P.F., Wynne, R.H., Oliphant, A.J., 2015a. Reconstructing disturbance history for an intensively mined region by time-series analysis of Landsat imagery. Environ. Monit. Assess. 187. http://dx.doi.org/10.1007/s10661-015-4766-1.

Li, X., Gong, P., Liang, L., 2015. A 30-year (1984–2013) record of annual urban dynamics of Beijing City derived from Landsat data. Remote Sens. Environ. 166, 78–90. http://dx.doi.org/10.1016/j.rse.2015.06.007.

Liang, L., Hawbaker, T.J., Chen, Y., Zhu, Z., Gong, P., 2014. Characterizing recent and projecting future potential patterns of mountain pine beetle outbreaks in the Southern Rocky Mountains. Appl. Geogr. 55, 165–175. http://dx.doi.org/10.1016/j.apgeog.2014.09.012.

Linke, J., McDermid, G.J., Laskin, D.N., McLane, a.J., Pape, A.D., Cranston, J., Hall-Beyer, M., Franklin, S.E., 2009. A disturbance-inventory framework for flexible and reliable landscape monitoring. Photogramm. Eng. Remote Sensing 75, 981–995. http://dx.doi.org/10.14358/PERS.75.8.981.

Liu, D., Cai, S., 2012. A spatial-temporal modeling approach to reconstructing land-cover change trajectories from multi-temporal satellite imagery. Ann. Assoc. Am. Geogr. 102, 1329–1347. http://dx.doi.org/10.1080/00045608.2011.596357.

Loveland, T.R., Dwyer, J.L., 2012. Landsat: building a strong future. Remote Sens. Environ. 122, 22–29. http://dx.doi.org/10.1016/j.rse.2011.09.022.

Lu, D., Mausel, P., Brondizio, E., Moran, E., 2004. Change detection techniques. Int. J. Remote Sens. 25 (12), 2365–2401.

Luo, Y., Trishchenko, A.P., Khlopenkov, K.V., 2008. Developing clear-sky, cloud and cloud shadow mask for producing clear-sky composites at 250-meter spatial resolution for the seven MODIS land bands over Canada and North America. Remote Sens. Environ. 112, 4167–4185. http://dx.doi.org/10.1016/j.rse.2008.06.010.

Margono, B.A., Turubanova, S., Zhuravleva, I., Potapov, P., Tyukavina, A., Baccini, A., Goetz, S., Hansen, M.C., 2012. Mapping and monitoring deforestation and forest degradation in Sumatra (Indonesia) using Landsat time series data sets from 1990 to 2010. Environ. Res. Lett. 7, 34010. http://dx.doi.org/10.1088/1748-9326/7/3/034010.

Markham, B.L., Helder, D.L., 2012. Forty-year calibrated record of earth-reflected radiance from Landsat: A review. Remote Sens. Environ. http://dx.doi.org/10.1016/j.rse.2011.06.026.

Marzen, L.J., Szantoi, Z., Harrington, L.M.B., Harrington, J.a., 2011. Implications of management strategies and vegetation change in the Mount St. Helens blast zone. Geocarto Int. 26, 359–376. http://dx.doi.org/10.1080/10106049.2011.584977.

Masek, J.G., Vermote, E.F., Saleous, N.E., Wolfe, R., Hall, F.G., Huemmrich, K.F., Lim, T. K., 2006. A Landsat surface reflectance dataset for North America, 1990–2000. IEEE Geosci. Remote Sens. Lett. 3 (1), 68–72.

Maxwell, S.K., Sylvester, K.M., 2012. Identification of "ever-cropped" land (1984–2010) using Landsat annual maximum NDVI image composites: Southwestern Kansas case study. Remote Sens. Environ. 121, 186–195. http://dx.doi.org/10.1016/j.rse.2012.01.022.

Meigs, G.W., Kennedy, R.E., Cohen, W.B., 2011. A Landsat time series approach to characterize bark beetle and defoliator impacts on tree mortality and surface fuels in conifer forests. Remote Sens. Environ. 115, 3707–3718. http://dx.doi.org/10.1016/j.rse.2011.09.009.

Meigs, G.W., Kennedy, R.E., Gray, A.N., Gregory, M.J., 2015. Spatiotemporal dynamics of recent mountain pine beetle and western spruce budworm outbreaks across the Pacific Northwest Region, USA. For. Ecol. Manage. 339, 71–86. http://dx.doi.org/10.1016/j.foreco.2014.11.030.

Mihai, B., Nistor, C., Simion, G., 2015. Post-socialist urban growth of Bucharest, Romania – a change detection analysis on Landsat imagery (1984–2010). Acta Geogr. Slov. 55, 223–234. http://dx.doi.org/10.3986/AGS.709.

Muttitanon, W., Tripathi, N.K., 2005. Land use/land cover changes in the coastal zone of Ban Don Bay, Thailand using Landsat 5 TM data. Int. J. Remote Sens. 26, 2311–2323. http://dx.doi.org/10.1080/01431160512331326666.

Neigh, C.S.R., Bolton, D.K., Williams, J.J., Diabate, M., 2014. Evaluating an automated approach for monitoring forest disturbances in the Pacific Northwest from logging, fire and insect outbreaks with landsat time series data. Forests 5, 3169–3198. http://dx.doi.org/10.3390/f5123169.

Nutini, F., Boschetti, M., Brivio, P.A., Bocchi, S., Antoninetti, M., 2013. Land-use and land-cover change detection in a semi-arid area of Niger using multi-temporal analysis of Landsat images. Int. J. Remote Sens. 34, 4769–4790. http://dx.doi.org/10.1080/01431161.2013.781702.

Oreopoulos, L., Wilson, M.J., Várnai, T., 2011. Implementation on landsat data of a simple cloud-mask algorithm developed for MODIS land bands. IEEE Geosci. Remote Sens. Lett. 8, 597–601. http://dx.doi.org/10.1109/LGRS.2010.2095409.

Palandro, D.A., Andréfouët, S., Hu, C., Hallock, P., Müller-Karger, F.E., Dustan, P., Callahan, M.K., Kranenburg, C., Beaver, C.R., 2008. Quantification of two decades of shallow-water coral reef habitat decline in the Florida Keys National Marine Sanctuary using Landsat data (1984–2002). Remote Sens. Environ. 112, 3388–3399. http://dx.doi.org/10.1016/j.rse.2008.02.015.

Palandro, D., Andréfouët, S., Muller-Karger, F.E., Dustan, P., Hu, C., Hallock, P., 2003. Detection of changes in coral reef communities using Landsat-5 TM and Landsat-7 ETM + data. Can. J. Remote Sens. 29, 201–209. http://dx.doi.org/10.5589/m02-095.

Pardo-Pascual, J.E., Almonacid-Caballer, J., Ruiz, L.A., Palomar-Vázquez, J., Rodrigo-Alemany, R., 2014. Evaluation of storm impact on sandy beaches of the Gulf of Valencia using Landsat imagery series. Geomorphology 214, 388–401. http://dx.doi.org/10.1016/j.geomorph.2014.02.020.

Parker, B.M., Lewis, T., Srivastava, S.K., 2015. Estimation and evaluation of multi-decadal fire severity patterns using Landsat sensors. Remote Sens. Environ. 170, 340–349. http://dx.doi.org/10.1016/j.rse.2015.09.014.

Pengra, B., Gallant, A., Zhu, Z., Dahal, D., 2016. Evaluation of the initial thematic output from a continuous change-detection algorithm for use in automated operational land-change mapping by the U.S. Geological Survey. Remote Sens. 8, 811. http://dx.doi.org/10.3390/rs8100811.

Pickell, P.D., Hermosilla, T., Coops, N.C., Masek, J.G., Franks, S., Huang, C., 2014. Monitoring anthropogenic disturbance trends in an industrialized boreal forest with Landsat time series. Remote Sens. Lett. 5, 783–792. http://dx.doi.org/10.1080/2150704X.2014.967881.

Pillay, K., Agjee, N.H., Pillay, S., 2014. Modelling changes in land cover patterns in Mtunzini, South Africa using satellite imagery. J. Indian Soc. Remote Sens. 42, 51–60. http://dx.doi.org/10.1007/s12524-013-0312-1.

Potapov, P., Turubanova, S., Hansen, M.C., 2011. Regional-scale boreal forest cover and change mapping using Landsat data composites for European Russia. Remote Sens. Environ. 115, 548–561. http://dx.doi.org/10.1016/j.rse.2010.10.001.

Potapov, P.V., Turubanova, S.A., Hansen, M.C., Adusei, B., Broich, M., Altstatt, A., Mane, L., Justice, C.O., 2012. Quantifying forest cover loss in Democratic Republic of the Congo, 2000–2010, with Landsat ETM + data. Remote Sens. Environ. 122, 106–116. http://dx.doi.org/10.1016/j.rse.2011.08.027.

Potapov, P.V., Turubanova, S.A., Tyukavina, A., Krylov, A.M., McCarty, J.L., Radeloff, V. C., Hansen, M.C., 2015. Eastern Europe's forest cover dynamics from 1985 to 2012 quantified from the full Landsat archive. Remote Sens. Environ. 159, 28–43. http://dx.doi.org/10.1016/j.rse.2014.11.027.

Powell, S.L., Cohen, W.B., Yang, Z., Pierce, J.D., Alberti, M., 2008. Quantification of impervious surface in the Snohomish Water Resources Inventory Area of Western Washington from 1972–2006. Remote Sens. Environ. 112, 1895–1908. http://dx.doi.org/10.1016/j.rse.2007.09.010.

Qiu, S., He, B., Zhu, Z., Liao, Z., Quan, X., 2017. Improving Fmask cloud and cloud shadow detection in mouantianous area for Landsats 4–8. Remote Sens. Environ. Accepted.

Ramadan, E., Feng, X., Cheng, Z., 2004. Satellite remote sensing for urban growth assessment in Shaoxing City, Zhejiang Province. J. Zhejiang Univ. Sci. 5, 1095–1101. http://dx.doi.org/10.1631/jzus.2004.1095.

Reiche, J., Verbesselt, J., Hoekman, D., Herold, M., 2015. Fusing Landsat and SAR time series to detect deforestation in the tropics. Remote Sens. Environ. 156, 276–293. http://dx.doi.org/10.1016/j.rse.2014.10.001.

Richter, R., 1997. Correction of atmospheric and topographic effects for high spatial resolution satellite imagery. Int. J. Remote Sens. 18, 1099–1111. http://dx.doi.org/10.1080/014311697218593.

Roy, D.P., Ju, J., Kline, K., Scaramuzza, P.L., Kovalskyy, V., Hansen, M., Loveland, T.R., Vermote, E., Zhang, C., 2010. Web-enabled Landsat Data (WELD): Landsat ETM + composited mosaics of the conterminous United States. Remote Sens. Environ. 114, 35–49. http://dx.doi.org/10.1016/j.rse.2009.08.011.

Roy, D.P., Ju, J., Lewis, P., Schaaf, C., Gao, F., Hansen, M., Lindquist, E., 2008. Multi-temporal MODIS-Landsat data fusion for relative radiometric normalization, gap filling, and prediction of Landsat data. Remote Sens. Environ. 112, 3112–3130. http://dx.doi.org/10.1016/j.rse.2008.03.009.

Roy, D.P., Kovalskyy, V., Zhang, H.K., Vermote, E.F., Yan, L., Kumar, S.S., Egorov, A., 2016. Characterization of Landsat-7 to Landsat-8 reflective wavelength and normalized difference vegetation index continuity. Remote Sens. Environ. 185, 57–70. http://dx.doi.org/10.1016/j.rse.2015.12.024.

Roy, D.P., Wulder, M.A., Loveland, T.R., C.E., W., Allen, R.G., Anderson, M.C., Helder, D., Irons, J.R., Johnson, D.M., Kennedy, R., Scambos, T.A., Schaaf, C.B., Schott, J.R., Sheng, Y., Vermote, E.F., Belward, A.S., Bindschadler, R., Cohen, W.B., Gao, F., Hipple, J.D., Hostert, P., Huntington, J., Justice, C.O., Kilic, A., Kovalskyy, V., Lee, Z. P., Lymburner, L., Masek, J.G., McCorkel, J., Shuai, Y., Trezza, R., Vogelmann, J., Wynne, R.H., Zhu, Z., 2014. Landsat-8: Science and product vision for terrestrial global change research. Remote Sens. Environ. 145, 154–172. http://dx.doi.org/10.1016/j.rse.2014.02.001.

Sader, S.A., Bertrand, M., Wilson, E.H., 2003. Satellite change detection of forest harvest patterns on an industrial forest landscape. For. Sci. 49, 341–353.

Sader, S.A., Legaard, K.R., 2008. Inclusion of forest harvest legacies, forest type, and regeneration spatial patterns in updated forest maps: A comparison of mapping results. For. Ecol. Manage. 255, 3846–3856. http://dx.doi.org/10.1016/j.foreco.2008.03.047.

Saunders, R.W., Kriebel, K.T., 1988. An improved method for detecting clear sky and cloudy radiances from AVHRR data. Int. J. Remote Sens. 9, 123–150. http://dx.doi.org/10.1080/01431168808954841.

Scaramuzza, P.L., Bouchard, M.A., Dwyer, J.L., 2012. Development of the landsat data continuity mission cloud-cover assessment algorithms. IEEE Trans. Geosci. Remote Sens. 50, 1140–1154. http://dx.doi.org/10.1109/TGRS.2011.2164087.

Schott, J.R., Gerace, A., Woodcock, C.E., Wang, S., Zhu, Z., Wynne, R.H., Blinn, C.E., 2016. The impact of improved signal-to-noise ratios on algorithm performance: Case studies for Landsat class instruments. Remote Sens. Environ. 185, 37–45. http://dx.doi.org/10.1016/j.rse.2016.04.015.

Schroeder, T.A., Wulder, M.A., Healey, S.P., Moisen, G.G., 2012. Detecting post-fire salvage logging from Landsat change maps and national fire survey data. Remote Sens. Environ. 122, 166–174. http://dx.doi.org/10.1016/j.rse.2011.10.031.

Schroeder, T.a., Cohen, W.B., Song, C., Canty, M.J.M.J., Yang, Z., Song, S., Canty, M.J.M. J., Zhiqiang, Y., 2006. Radiometric correction of multi-temporal Landsat data for charecterization of early successional forest patterns in western Oregon. Remote Sens. Environ. 103, 16–26. http://dx.doi.org/10.1016/j.rse.2006.03.008.

Senf, C., Pflugmacher, D., Wulder, M.A., Hostert, P., 2015. Characterizing spectral-temporal patterns of defoliator and bark beetle disturbances using Landsat time series. Remote Sens. Environ. 170, 166–177. http://dx.doi.org/10.1016/j.rse.2015.09.019.

Sieber, A., Kuemmerle, T., Prishchepov, A.V., Wendland, K.J., Baumann, M., Radeloff, V.C., Baskin, L.M., Hostert, P., 2013. Landsat-based mapping of post-Soviet land-use change to assess the effectiveness of the Oksky and Mordovsky protected areas in European Russia. Remote Sens. Environ. 133, 38–51. http://dx.doi.org/10.1016/j.rse.2013.01.021.

Singh, A., 1989. Digital change detection techniques using remotely-sensed data. Int. J. Remote Sens. 10, 989–1003. http://dx.doi.org/10.1080/01431168908903939.

Song, C., Woodcock, C.E., 2003. Monitoring forest succession with multitemporal landsat images: factors of uncertainty. IEEE Trans. Geosci. Remote Sens. 41, 2557–2567. http://dx.doi.org/10.1109/TGRS.2003.818367.

Song, C., Woodcock, C.E., Seto, K.C., Lenney, M.P., Macomber, S.A., 2001. Classification and change detection using Landsat TM data: When and how to correct atmospheric effects? Remote Sens. Environ. 75, 230–244. http://dx.doi.org/10.1016/S0034-4257(00)00169-3.

Sonnenschein, R., Kuemmerle, T., Udelhoven, T., Stellmes, M., Hostert, P., 2011. Differences in Landsat-based trend analyses in drylands due to the choice of vegetation estimate. Remote Sens. Environ. 115, 1408–1420. http://dx.doi.org/10.1016/j.rse.2011.01.021.

Su, Z., 2000. Remote sensing of land use and vegetation for mesoscale hydrological studies. Int. J. Remote Sens. 21, 213–233. http://dx.doi.org/10.1080/014311600210803.
Sulla-Menashe, D., Friedl, M.A., Woodcock, C.E., 2016. Sources of bias and variability in long-term Landsat time series over Canadian boreal forests. Remote Sens. Environ. 177, 206–219. http://dx.doi.org/10.1016/j.rse.2016.02.041.
Thonfeld, F., Hecheltjen, A., Menz, G., 2015. Bi-temporal change detection, change trajectories and time series analysis for forest monitoring. Photogramm. - Fernerkundung - Geoinf. 2015, 129–141. http://dx.doi.org/10.1127/pfg/2015/0259.
Tulbure, M.G., Broich, M., 2013. Spatiotemporal dynamic of surface water bodies using Landsat time-series data from 1999 to 2011. ISPRS J. Photogramm. Remote Sens. 79, 44–52. http://dx.doi.org/10.1016/j.isprsjprs.2013.01.010.
Unger, D., Hung, I.-K., Farrish, K., Dans, D., 2015. Quantifying land cover change due to petroleum exploration and production in the Haynesville shale region using remote sensing. Int. J. Appl. Geospatial Res. 6, 1–17. http://dx.doi.org/10.4018/ijagr.2015040101.
Verbesselt, J., Hyndman, R., Zeileis, A., Culvenor, D., 2010. Phenological change detection while accounting for abrupt and gradual trends in satellite image time series. Remote Sens. Environ. 114, 2970–2980. http://dx.doi.org/10.1016/j.rse.2010.08.003.
Verbesselt, J., Zeileis, A., Herold, M., 2012. Near real-time disturbance detection using satellite image time series. Remote Sens. Environ. 123, 98–108. http://dx.doi.org/10.1016/j.rse.2012.02.022.
Vermote, E., Justice, C., Claverie, M., Franch, B., 2016. Preliminary analysis of the performance of the Landsat 8/OLI land surface reflectance product. Remote Sens. Environ. 185, 46–56. http://dx.doi.org/10.1016/j.rse.2016.04.008.
Vermote, E., Saleous, N., 2007. LEDAPS surface reflectance product description 1–21.
Vermote, E.F., Tanré, D., Deuzé, J.L., Herman, M., Morcrette, J.J., 1997. Second simulation of the satellite signal in the solar spectrum, 6 s: an overview. IEEE Trans. Geosci. Remote Sens. 35, 675–686. http://dx.doi.org/10.1109/36.581987.
Vogelmann, J.E., Gallant, A.L., Shi, H., Zhu, Z., 2016. Perspectives on monitoring gradual change across the continuity of Landsat sensors using time-series data. Remote Sens. Environ. 185, 258–270. http://dx.doi.org/10.1016/j.rse.2016.02.060.
Vogelmann, J.E., Gallant, A.L., Shi, H., Zhu, Z., 2015. Perspectives on monitoring gradual change across the continuity of Landsat sensors using time-series data. Remote Sens. Environ. http://dx.doi.org/10.1016/j.rse.2016.02.060.
Vogelmann, J.E., Xian, G., Homer, C., Tolk, B., 2012. Monitoring gradual ecosystem change using Landsat time series analyses: Case studies in selected forest and rangeland ecosystems. Remote Sens. Environ. 122, 92–105. http://dx.doi.org/10.1016/j.rse.2011.06.027.
Vorovencii, I., 2014. A change vector analysis technique for monitoring land cover changes in Copsa Mica, Romania, in the period 1985–2011. Environ. Monit. Assess. 186, 5951–5968. http://dx.doi.org/10.1007/s10661-014-3831-5.
Wang, B., Ono, A., Muramatsu, K., Fujiwara, N., 1999. Automated detection and removal of clouds and their shadows from landsat TM images. Ieice Trans. Inf. Syst. E82D, 453–460.
White, J.C., Wulder, M.A., Hobart, G.W., Luther, J.E., Hermosilla, T., Griffiths, P., Coops, N.C., Hall, R.J., Hostert, P., Dyk, A., Guindon, L., 2014. Pixel-based image compositing for large-area dense time series applications and science. Can. J. Remote Sens. 40, 192–212. http://dx.doi.org/10.1080/07038992.2014.945827.
Wilson, E.H., Sader, S.A., 2002. Detection of forest harvest type using multiple dates of Landsat TM imagery. Remote Sens. Environ. 80, 385–396. http://dx.doi.org/10.1016/S0034-4257(01)00318-2.
Woodcock, C., E.A., 2008. 1018 Free Access to Landsat Imagery Teach by the Book Science Education : Science (80-.). 320, 1011–1012. http://dx.doi.org/10.1126/science.320.5879.1011a.
Wulder, M.A., Masek, J.G., Cohen, W.B., Loveland, T.R., Woodcock, C.E., 2012. Opening the archive: How free data has enabled the science and monitoring promise of Landsat. Remote Sens. Environ. 122, 2–10. http://dx.doi.org/10.1016/j.rse.2012.01.010.
Wulder, M.A., White, J.C., Loveland, T.R., Woodcock, C.E., Belward, A.S., Cohen, W.B., Fosnight, E.A., Shaw, J., Masek, J.G., Roy, D.P., 2016. The global Landsat archive: Status, consolidation, and direction. Remote Sens. Environ. 185, 271–283. http://dx.doi.org/10.1016/j.rse.2015.11.032.
Xue, X., Liu, H., Mu, X., Liu, J., 2014. Trajectory-based detection of urban expansion using Landsat time series. Int. J. Remote Sens. 35, 1450–1465. http://dx.doi.org/10.1080/01431161.2013.878058.
Yang, Y., Zhang, S., Wang, D., Yang, J., Xing, X., 2015. Spatiotemporal changes of farming-pastoral ecotone in Northern China, 1954–2005: A case study in Zhenlai County, Jilin Province. Sustain. 7, 1–22. http://dx.doi.org/10.3390/su7010001.
Zanotta, D.C., Bruzzone, L., Bovolo, F., Shimabukuro, Y.E., 2015. An adaptive semisupervised approach to the detection of user-defined recurrent changes in image time series. IEEE Trans. Geosci. Remote Sens. 53, 3707–3719. http://dx.doi.org/10.1109/TGRS.2014.2381645.
Zeileis, A., Leisch, F., Kleiber, C., Hornik, K., 2005. Monitoring structural change in dynamic econometric models. J. Appl. Econom. 20, 99–121. http://dx.doi.org/10.1002/jae.776.
Zhang, H., Qi, Z.fang, Ye, X.yue, Cai, Y.bin, Ma, W.chun, Chen, M.nan, 2013. Analysis of land use/land cover change, population shift, and their effects on spatiotemporal patterns of urban heat islands in metropolitan Shanghai. China. Appl. Geogr. 44, 121–133. http://dx.doi.org/10.1016/j.apgeog.2013.07.021.
Zhang, H.K., Roy, D.P., 2016. Landsat 5 Thematic Mapper reflectance and NDVI 27-year time series inconsistencies due to satellite orbit change. Remote Sens. Environ. 186, 217–233. http://dx.doi.org/10.1016/j.rse.2016.08.022.
Zhao, J., Guo, W., Huang, W., Huang, L., Zhang, D., Yang, H., Yuan, L., 2014. Characterizing spatiotemporal dynamics of land cover with multi-temporal remotely sensed imagery in Beijing during 1978–2010. Arab. J. Geosci. 7, 3945–3959. http://dx.doi.org/10.1007/s12517-013-1072-5.
Zhu, X., Chen, J., Gao, F., Chen, X., Masek, J.G., 2010. An enhanced spatial and temporal adaptive reflectance fusion model for complex heterogeneous regions. Remote Sens. Environ. 114, 2610–2623. http://dx.doi.org/10.1016/j.rse.2010.05.032.
Zhu, Z., Fu, Y., Woodcock, C.E., Olofsson, P., Vogelmann, J.E., Holden, C., Wang, M., Dai, S., Yu, Y., 2016a. Including land cover change in analysis of greenness trends using all available Landsat 5, 7, and 8 images: A case study from Guangzhou, China (2000–2014). Remote Sens. Environ. 185, 243–257. http://dx.doi.org/10.1016/j.rse.2016.03.036.
Zhu, Z., Gallant, A.L., Woodcock, C.E., Pengra, B., Olofsson, P., Loveland, T.R., Jin, S., Dahal, D., Yang, L., Auch, R.F., 2016b. Optimizing selection of training and auxiliary data for operational land cover classification for the LCMAP initiative. ISPRS J. Photogramm. Remote Sens. 122, 206–221. http://dx.doi.org/10.1016/j.isprsjprs.2016.11.004.
Zhu, Z., Wang, S., Woodcock, C.E., 2015a. Improvement and expansion of the Fmask algorithm: Cloud, cloud shadow, and snow detection for Landsats 4–7, 8, and Sentinel 2 images. Remote Sens. Environ. 159, 269–277. http://dx.doi.org/10.1016/j.rse.2014.12.014.
Zhu, Z., Woodcock, C.E., 2014a. Continuous change detection and classification of land cover using all available Landsat data. Remote Sens. Environ. 144, 152–171. http://dx.doi.org/10.1016/j.rse.2014.01.011.
Zhu, Z., Woodcock, C.E., 2014b. Automated cloud, cloud shadow, and snow detection in multitemporal Landsat data: An algorithm designed specifically for monitoring land cover change. Remote Sens. Environ. 152, 217–234. http://dx.doi.org/10.1016/j.rse.2014.06.012.
Zhu, Z., Woodcock, C.E., 2012. Object-based cloud and cloud shadow detection in Landsat imagery. Remote Sens. Environ. 118, 83–94. http://dx.doi.org/10.1016/j.rse.2011.10.028.
Zhu, Z., Woodcock, C.E., Holden, C., Yang, Z., 2015b. Generating synthetic Landsat images based on all available Landsat data: Predicting Landsat surface reflectance at any given time. Remote Sens. Environ. 162, 67–83. http://dx.doi.org/10.1016/j.rse.2015.02.009.
Zhu, Z., Woodcock, C.E., Olofsson, P., 2012. Continuous monitoring of forest disturbance using all available Landsat imagery. Remote Sens. Environ. 122, 75–91. http://dx.doi.org/10.1016/j.rse.2011.10.030.